REMOTE SENS. ENVIRON. 29:27–52 (1990)

Vegetation in Deserts: II. Environmental Influences on Regional Abundance

Milton O. Smith, Susan L. Ustin, John B. Adams, and Alan R. Gillespie*

*Department of Geological Sciences, University of Washington, Seattle and *Department of Land, Air, and Water Resources, University of California, Davis*

A remote-sensing approach was used in conjunction with field measurements to examine local and regional-scale environmental processes that covary with the abundance and distribution of vegetation in a semiarid ecosystem. Images of the fractional abundances of vegetation and soils were constructed by spectral mixture analysis of Landsat Thematic Mapper (TM) satellite images, covering a 150-km segment of Owens Valley, California. These images, along with a TM image of the radiant temperature, a digital elevation image and ground-based measurements of precipitation and evapotranspiration, were examined to isolate the effects on vegetation of the covarying factors, net radiation, temperature, elevation, soil type, and precipitation. On a regional scale the abundance of desert scrub on the bajadas of Owens Valley appears to be influenced most by the mean annual precipitation. Also regionally, vegetation cover is sensitive to the differences between the gravelly fanglomerates of the bajadas and the alluvium of the valley floor. Other edaphic and ground-water effects are important but localized, and are most pronounced on the valley floor. They produce patterns in vegetation abundance that are independent of and superposed on the regional precipitation-controlled pattern. Temperature covaries with vegetation less well than precipitation, and appears not to be the major influence on either the amount of vegetation or the boundaries between major vegetation communities. The image-derived measure of vegetation cover correlates closely with ground-based measurements of evapotranspiration. The study demonstrates that local observations cannot be extrapolated safely to the regional scale, and that a combination of local field measurements and the regional measurements provided by remote sensing is required to determine the environmental factors that control vegetation distribution.

INTRODUCTION

This paper is Part II of a two-part study of desert vegetation, focused on Owens Valley, California [Fig. 1a)]. In Part I (Smith et al., this issue) we showed how remotely sensed measurements could be used to estimate vegetation abundance in semiarid and arid deserts. In Part II we analyze how the environmental factors of net radiation (R_n), temperature (T_s), elevation, precipitation, and soil type affect vegetation abundance in a semiarid landscape. Previously, the relationships between vegetation abundance and these covarying factors have been obscured by inadequate spatial and temporal sampling. Data have been collected at

Address correspondence to Dr. Milton O. Smith, Dep. of Geological Sci., AJ-20, Univ. of Washington, Seattle, WA 98195.
Received 19 October 1989; revised 21 February 1990.

0034-4257/90/$3.50

655 Avenue of the Americas, New York, NY 10010

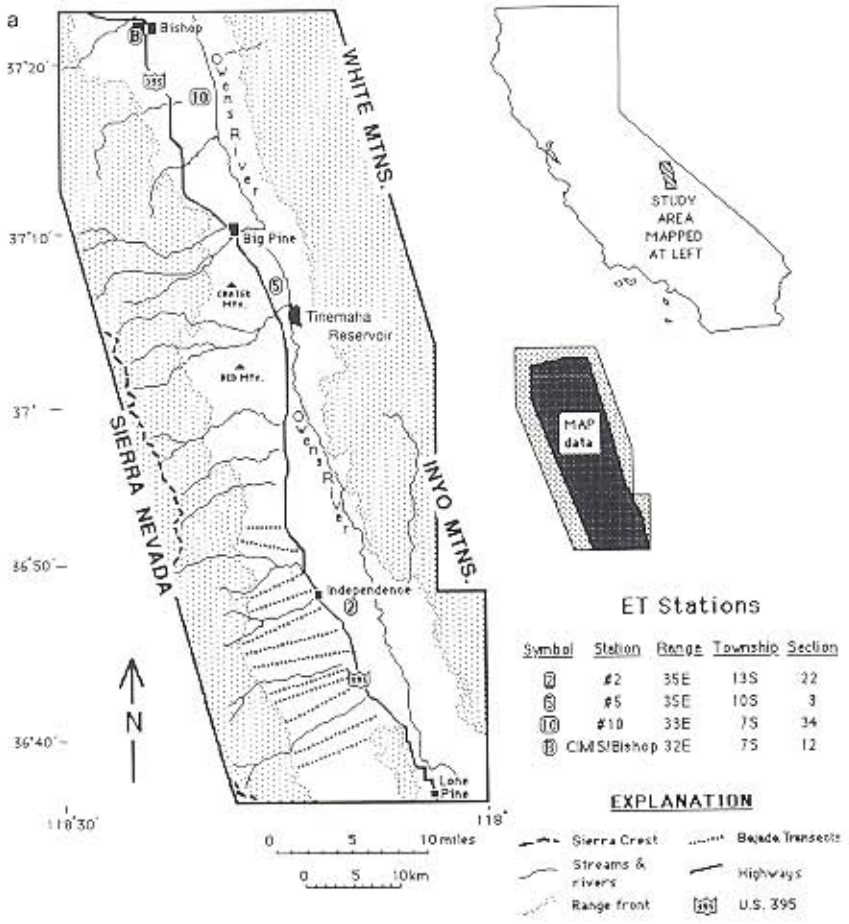

Figure 1. Index maps showing Owens Valley. Map outlines correspond to the TM data coverage. a) Geographic names, data stations, and bajada transects. Mountains are stippled. Reduced-scale map at right shows area for which mean annual precipitation (MAP) data were available. b) Major vegetation communities, based on unpublished data from the Benton–Owens Valley Area Soil Survey (U.S.D.A. Soil Conservation Service, Bishop, CA). The vegetation communities outside the boundaries of Bureau of Land Management land on the upper bajadas and foothills are mapped from aerial photographs.

points, but interpreted to have regional significance. The data describing conditions at local scales may not apply regionally because 1) the environment may be different outside of the area of measurement, 2) the coupling of environmental factors may vary with scale, and 3) community-based classifications of vegetation may be inappropriate for characterizing the regional ecosystem.

As an example of the scaling problem, Jarvis and McNaughton (1986) pointed out that predicting regional evapotranspiration requires more than extending local models to landscapes. They showed that, at the scale of the leaf or the plant, evapotranspiration (ET) is effectively regulated by stomatal conductance, but at the regional scale net radiation and average temperature are the controlling factors. Stomatal regulation at the level of individual leaves leads to compensating microclimatic feedbacks at the community level. Measurements of stomatal conductance are not sufficient to estimate ET at the community level.

Satellite multispectral images are now beginning to be applied to ecological studies (e.g., Waring et al., 1986). Because digital images consist of massively repetitive discrete spatial measurements, they potentially provide one way to extend information from local to regional scales. Data from several Earth-observing satellites are presently available, and new systems are under development.

Satellite measurements have potential for depicting parameters such as R_n and T_s, as well as other parameters relating to the interaction of electromagnetic radiation and the Earth's surface. However, this potential can be realized only if the physical significance of the remote measurements is established ecologically. Thus, for example, it may be significant to determine the percent cover of green vegetation for an area on the ground, but it is not of direct value to the ecologist to know the radiance at various wavelengths for the same area. The statistical classifications and correlations that commonly are used on multispectral images are performed on the radiance or reflectance data, and, lacking a physical basis by themselves, are not sufficient to connect the satellite measurements to materials and conditions on the ground.

In the present study Landsat Thematic Mapper (TM) satellite data and field measurements from Owens Valley, a region encompassing the transition between the Mojave and Great Basin deserts [Fig. 1b)], are used to examine environmental patterns at several spatial scales. The satellite measures scene radiance in six different spectral bands in the visible and near-infrared wavelength regions, and one band in the thermal-infrared region. Radiance values in the visible and near-infrared regions respond to variations in the chemistry and structure of materials at the Earth's surface, but they may not respond directly to the same parameters that an ecologist would measure in the field, such as vegetation cover, soil moisture, or community composition. In the field and laboratory most plant species and communities are identified by morphological rather than chemical criteria, and the resolution of a single (30 m × 30 m) TM picture element (pixel) is far too coarse for direct morphological identification (Part I). Aggregates of species may be identified from satellite images if they possess unique reflectance spectra, but this is not often the case. More typically, species are inferred from spatial and/or temporal patterns and from context.

In Part I we described a method for analyzing Landsat images that isolated the spectral radiance contributions of vegetation, soil, and shade in the pixel data. Radiance measurements from the six visible and near-infrared image channels were mathematically transformed into the relative fractions of a few endmember spectra which, when mixed together, accounted for the observed spectral variation in the scene. Using this spectral-mixture framework, we then mapped the relative abundances of two vegetation and two soil types in Owens Valley. The goal of Part II, the present paper, is to examine the relationship of the scaled vegetation fraction (VF_s) measured by Smith et al. (1990) to five environmental factors: net radiation (R_n); radiant temperature (T_s); elevation; mean annual precipitation (MAP); and soil type. All of these environmental factors can be determined and expressed in image form along with the vegetation abundance, using a TM image, reference spectra, ground-based meteorological data, and digital elevation images. We examine and compare these spatial data sets, and test whether local correlations among environmental parameters that have been documented in the field extend to regional scales. We then use the spatial patterns of the observed regional gradients to assess to what extent each of the factors affects the distribution and abundance of vegetation.

A specific objective in Part II is to determine whether temperature, water (soil moisture), or soil composition has a dominant effect on the abundance and distribution of vegetation in Owens Valley. Soil nutrients, moisture, and temperature have all been implicated as limiting vegetation resources in semiarid lands (among others, see Merriam, 1898; Billings, 1949; Shelford, 1963; Beatley, 1974; 1975; Schreve, 1912; 1934; West, 1983a, b, c; MacMahon and Wiebolt, 1978; MacMahon and Wagner, 1985). Some authors stress the significance of minimum/maximum air temperatures in winter and summer in controlling the distribution of semiarid vegetation, or utilize day-degrees (integrating temperature over time) as factors to separate vegetation zones (Hastings and Turner, 1965). Scrub cover has been shown to be proportional to precipitation in some semiarid regions (Beatley, 1974; 1975; Goldberg and Turner, 1986), and a review by Shimeda (1985) concludes that Leaf-Area Index (LAI) and productivity are generally proportional to precipitation.

A high correlation among precipitation, vegetation cover, and elevation commonly has been observed in semiarid landscapes. Because precipitation varies with both air temperature and elevation, it has been difficult to isolate the effects of each on plant distribution. Previous studies have relied on extensive temporal sampling and have involved only limited spatial sampling. For example, Beatley (1974) concluded that minimum daily air temperatures control the transition between the vegetation communities of the Mojave and Great Basin deserts, based on relatively limited spatial/temporal data acquired at local scales. We argue that causal relationships among these interrelated parameters may best be revealed on a regional scale, by correlation of spatial patterns of variability in registered maps and images of VF_s and the candidate driving parameters. Using the TM images, we can study vegetation distribution and abundance using a 100%-sampled spatial data base.

Soil moisture cannot be measured directly by TM; however, we hypothesize that if the abundance of green vegetation (which we derived from the six-band radiance data) is an indication of availability of soil moisture, then the vegetation fraction (VF_s) and related spectral parameters are indirect measures of evapotranspiration (ET), integrated over a period of time characteristic of the vegetation community. These hypotheses are tested in terms of ground micrometeorological measurements and the patterns in the image data.

METHODS

The research strategy was to analyze satellite image data in the visible, near-infrared, and thermal-infrared spectral regions in terms of spectral mixtures of vegetation and soil. These measurements were combined with conventional parametersdescribing net radiation and radiant temperature. Vegetation fractions were compared with field measurements of vegetation cover (Part I). Other data were acquired from reported ground-based observations and measurements, compiled into image or map format: these data include the distribution of vegetation communities, digital elevation images, soil temperatures, and mean annual precipitation.

Remotely measured radiant temperature is mixed from substrate and vegetation temperatures. Substrate temperatures are proportional, among other things, to the net solar radiation absorbed by the surface, whereas the vegetation temperatures are more dependent upon air temperature and evaporative cooling. Images of the net radiation and radiant temperature data were compared in an effort to understand whether the substrate or vegetation is the significant factor controlling radiant temperature.

Correlations of soil type and vegetation cover were investigated by visual inspection of images showing the proportions of desert scrub and of young, poorly developed soil. Correlations of vegetation cover and the other parameters were examined in three ways: 1) linear regressions of each parameter to elevation were compared; 2) the gross correlations of vegetation cover, temperature, and precipitation to elevation were removed from the images and the residual images were compared; and 3) the gross correlations of vegetation cover to temperature and to precipitation were removed from the images, and the residual images were compared using color-coded contour maps.

Correlations of vegetation cover, temperature, and precipitation with elevation were established by regression of the image data and spatially registered digital elevation data sets along selected

transects (discussed below). New images of estimated vegetation cover, temperature, and precipitation were calculated from the regression coefficients and the elevation images. The gross correlations were then removed from the reduced data by subtracting these estimated images from the vegetation cover, temperature, and precipitation images, respectively. The subtracted data form residual images that highlight local departures from the regional correlation with elevation. A similar protocol was followed in calculating residual images of vegetation cover regressed to temperature and to precipitation. Finally, the satellite estimates of vegetation cover were regressed to local evapotranspiration values estimated from field measurements.

Satellite Image Data

The TM data used in this analysis were acquired on 16 May 1985 at approximately 09:50 PST (Landsat 5: Path 41, Rows 34 and 35). Net radiation (R_n) was calculated from TM Bands 1–5 and 7, together spanning the visible and near-infrared spectral regions (0.48–2.3 μm), using the weighted-average method of Jackson (1984) and Jackson et al. (1985). TM Bands 1–5 and 7 are acquired in 30 m × 30 m pixels.

TM Band 6, which is the thermal-infrared spectral region (10.4–12.5 μm), was used to determine the distribution of radiant surface temperatures (T_s) for the entire Owens Valley. T_s was calculated using an assumed emittance value of 0.95 (Sellers, 1965; Price, 1981). The thermal radiance data were calibrated using coefficients supplied by NASA; the resolution is ~0.5°C. TM Band 6 is acquired in 120 m × 120 m pixels.

The TM data were also used to determine spectral endmembers and fraction images as described by Smith et al. (1990). The endmembers included two types of soil, vegetation and shade. Endmember fractions were rescaled to normalize for shade. Soil type was inferred from the rescaled soil-fraction images, and vegetation cover was estimated from VF_s, the rescaled vegetation fraction (Part I).

Elevation Data

Elevation data were taken from a USGS digital terrain map based upon 1:250,000-scale topographic maps with 200-ft (~61 m) contour intervals and reported with quantum intervals of 1 ft (~0.3 m) and approximate accuracy of ±20 ft (~6 m). The pixel size is ~64 m × 64 m, roughly comparable to the TM data. These data are in image format and were geometrically registered to the TM images to facilitate comparison.

Soil and Air Temperature Distributions

Mean annual and mean summer soil temperatures (MAST and MSST) have been measured for field stations in Nevada by Schmidlin et al. (1983). These measurements were regressed against elevation and summarized as linear equations relating elevation and soil temperatures. These equations, which contain a term proportional to latitude, are generally applicable to much of the Great Basin, but measured values from sites in western Nevada are reported to be ~1°C lower than predicted. The latitude term predicts a linear decrease of 0.8°C from Lone Pine to Bishop [Fig. 1a)], for a given elevation.

MAST and MSST have been measured for a 5-year period for sites within Owens Valley by the Soil Conservation Service (E. Tallyn, personal communication, 1987). These data show the same trends with elevation as those reported for Nevada, but they are ~2°C lower than predicted by the equations. Maps of measured MAST and MSST are not available for Owens Valley.

Air temperatures for Owens Valley have been measured at a number of stations, some for as long as 80 years (Hollett et al., 1988). Mean monthly and annual temperatures have been calculated for these stations, but a regional map of these data for Owens Valley has not yet been compiled.

Precipitation Distribution

Mean annual precipitation (MAP) values have been calculated from rainfall collected during the years 1930–1986 at 21 rain gauges irregularly distributed over the bajadas and floor of Owens Valley (Hollett et al., 1988). These data have been generalized as an isohyctal contour map, which lacks the high spatial resolution of the TM images. Comparable maps depicting seasonal and annual variability are not currently available. We calculated a MAP image by linear interpolation be-

tween the contours of the isohyetal map in order to match the TM scale.

False-Color Image of T_s, VF_s, and MAP

The spatial correlations among T_s, VF_s, and MAP were analyzed by constructing a color-coded VF_s image (cf. Part I, Fig. 6) upon which was superposed a single differently color-coded and smoothed T_s isotherm. These colored data were displayed over a black/white "complemented" shade fraction image [Part I, Fig. 4a)], which displays the topography for reference. Separately superposed over the VF_s and shade images was a single color-coded MAP isohyet. Inspection of the patterns of variation among the correlated parameters is possible using this image, and is a sensitive method of assessing the consistency of covariance calculated by local regression at points or isolated transects. We anticipate that causal relationships among the many covarying parameters will be revealed by the consistent spatial patterns of variation in the images. In particular, we hope to determine from the concordance or discordance of the contour lines whether vegetation cover is controlled by temperature, by precipitation, or by both.

Temperature, Vegetation, and Precipitation Transects

Precipitation, soil temperature, and vegetation community and cover are all correlated with elevation, and thus it is likely that T_s, VF_s, MAP, and elevation are also all highly correlated across the Sierran bajada. Elevation appears to be the chief independent variable among those under study. We therefore separately regressed each variable against elevation, to reduce the high degree of correlation among the parameters of interest.

The regressions were done for data from 12 transects on the bajada [Fig. 1a)]. These transects were along east–west slopes on the Sierran alluvial fans for which soil type and development were constant, and for which the range of elevations was $\leqslant$500 m. A linear relationship was hypothesized, of the form $P = a - bE$, where P is the dependent parameter, E is the elevation in meters, and a and b are empirical coefficients. For each transect, values of the P (T_s, VF_s, and MAP) were regressed to the values of E to determine a and b. Using the above equation with these coefficients, images of estimated P ($\hat{P}$) were calculated, pixel by pixel, from the elevation image.

Residual Images

In order to compare actual distributions of P with those predicted from elevation alone, residual images of $P - \hat{P}$ were calculated for T_s, VF_s, and MAP. The residual image for precipitation was much more generalized than the others. All three residual images are insensitive to covariance with elevation, and highlight areas where less covariance is observed. The $MAP - \overline{MAP}$ residual image was displayed as a color-coded contour map "draped" over the complemented shade fraction image.

We also calculated residual images depicting vegetation cover regressed to T_s and to MAP. These images present a different view of the covarying parameters in which the relationships between vegetation and temperature or precipitation are directly expressed. They were displayed as color-coded contour maps "draped" over the complemented shade fraction image.

Ground Station ET Measurements

A daily estimate of ET on the date of image acquisition was obtained from four locations on the valley floor [Fig. 1a)]. For three of the four locations (Stations #2, 5, and 10) hourly measurements of net radiation (R_n), air temperature, soil temperature, relative humidity, wind speed, and other standard micrometerological parameters were made by the USGS. We obtained the measurements for the entire month of May 1985. These data were used to calculate daily ET using standard methods for eddy correlation (unpublished data from L. Duell, USGS, San Diego). Station #2 is located near the town of Independence in an alkali sacaton, saltgrass, and baltic rush meadow. Station #5 is located northwest of Tinemaha Reservoir in a greasewood, shadscale, Nevada saltbush, and sagebrush mixed-desert scrub. Station #10 is located southeast of the town of Bishop in a greasewood, shadscale, and Nevada-saltbush scrub.

Inspection of all the daily ET for the month of May 1985 sites show that the values were consistent with each other within ± 1 mm at the three sites. The Bowen ratio, eddy correlation, and

Penman–Monteith methods were used to calculate daily ET for four days (2–5 June, 1986), and the results agreed within ±1.5 mm (Wilson et al., 1989). This level of agreement is acceptable for estimates of daily ET for sparse vegetation in a heterogeneous arid habitat, and we think that it provides a good estimate of the precision of the techniques.

Daily ET for the fourth site, the Bishop Station of CIMIS, the California Irrigation Management Information System [Fig. 1a)], was estimated using hourly data measured above a standard grass surface and summed for every 24-h period. CIMIS uses a modified Penman equation to calculate energy budget parameters (George et al., 1985; Snyder and Pruitt, 1985). For the Bishop Station, estimates of daily ET for the 2-week period around TM image acquisition varied within the range 7–9 mm. Estimates of average daily ET for May, made using four different techniques, agreed within 2.4 mm over the period 1985–1987 (Smith, 1987). These data afford a reasonable approximation to the precision of the daily ET estimates.

Annual ET estimates were available from the Los Angeles Department of Water and Power for 112 land units within the USGS Independence, CA 7.5-min quadrangle map. Rawson and colleagues (R. Rawson, personal communication, 1989) and Groeneveld et al. (1986; personal communication, 1989) used the map units with transpiration and climate models developed for Owens Valley, in order to calculate annual ET estimates for each parcel. Vegetation was classified according to community from air photos and field surveys and line intercept transects were used to calculate percentage canopy cover in each parcel (P. Novak, unpublished data on file with the Los Angeles Department of Water and Power). We used this information to merge units having similar ET values and the same vegetation community into 32 grouped land units for comparison with remotely sensed vegetation cover estimates.

Vegetation cover for the ET stations was calculated from the image data for comparison to the ET estimates. A 4×4 pixel (120 m×120 m) window covering each of stations #2, 5, and 10 was extracted from the VF_s image. The grass field at the CIMIS station was itself only 8 m×12 m, smaller than a TM pixel. However, it was surrounded by an irrigated pasture roughly 40 m×40 m in size, and the VF_s of the pixel encompassing the station is close to correct. Thus averaging a 4×4 pixel window was inappropriate, and the maximum value of VF_s from the 4×4 pixel window was used instead. Even so, VF_s for the CIMIS station may be a minimum value. VF_s values associated with the annual ET were averaged over polygonal regions in the image corresponding to the land units used to estimate ET. The area of these polygons was typically ~5000 pixels.

Variation diagrams were constructed relating the estimates of daily and annual ET to the calibrated VF_s estimates of cover. The correlation was quantified by regressing ET to the vegetation cover estimates.

RESULTS

Net Radiation

The image of R_n is shown in Figure 2, which closely resembles a "negative" of the visible and near-infrared TM images, or the "shade" fraction image of Part I. R_n is a measure of the radiant flux absorbed in the scene; thus it is responsive predominantly to topographic shadowing, and to photometric shading. It also is responsive to shade due to subpixel objects such as boulders and trees, and albedo differences due to vegetation and to variations in soils and exposed rocks. All these effects may be seen in Figure 2. Because of shade and the southeastern solar azimuth, northern and western slopes are light, and southern and eastern slopes are dark. This imparts a sense of topography to the image that is its dominant feature. Subpixel shadows, plus the low albedo of vegetation, lighten the Sierran bajada, except where there are sparsely vegetated range-fire scars, which are dark in Figure 2. Densely vegetated riparian zones along streams and in the valley floor are light. Low-albedo basalt flows are light, and reflective snow fields in the Sierra Nevada and salt flats on the valley floors are dark.

Radiant Temperature

The image of T_s, acquired simultaneously with R_n, is shown in Figure 3. Weather conditions on the date of image acquisition were stable with clear skies, and were similar to those of the preceding days. Thus the radiant temperatures shown

in Figure 3 have not been influenced significantly by soil moisture. Major tonal patterns are associated primarily with elevation, with the exception of lakes and other bodies of water. Tones in the mountains are dark (cool), especially where there is snow at higher elevations in the Sierra Nevada. The bajadas and valley floor are light (warm), in part because the denser air retards radiative heat loss.

Temperature contrast is minimal on the bajada surface, which typically consists of bouldery granitic gravels under a 10–30% cover of desert scrub (Part I). The greatest contrast on the alluvial fans occurs not among surfaces with different lithologies, but among areas of different vegetation cover. Most noticeable is the contrast between the lighter, sparsely vegetated distal ends (~27°C) and the darker, more vegetated upper regions (~22°C) of the fans west of Independence [Fig. 1a]. To a lesser degree, the darker fans and the lighter, less vegetated fire scars on the same surface also contrast (e.g., ~19° vs. ~24°C).

Basalt flows from two volcanoes, Crater Mountain and Red Mountain, are somewhat lighter than the rest of the bajada, if similar slopes are compared. The thermal contrast between the low-albedo lavas and the high-albedo granitic alluvium is generally <5°C, however. The contact between basalt and granitic alluvium in one recent fire scar is difficult to detect (~1°C). Obviously, the vege-

Figure 2. Net radiation (R_n) image calculated from TM data. Major geographic features in Figures 2–11 are labelled in Part I, Figure 4a).

Figure 3. Radiant temperature (T_r) image calculated from TM data.

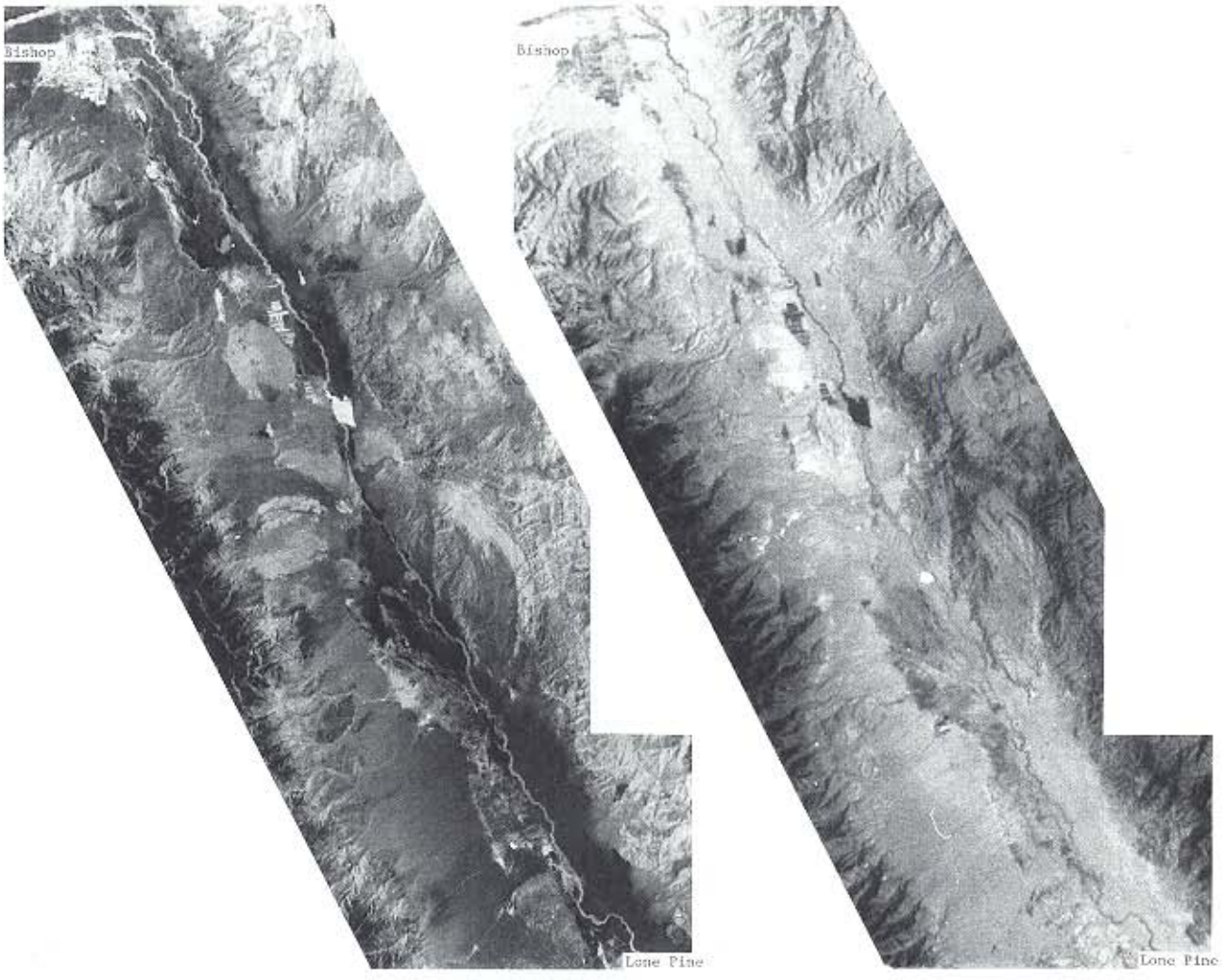

tation exerts a dominant influence on radiant temperature at the scale of TM data.

The areas of greatest thermal contrast within the lavas are the sun-facing (~33°C) and shadowed (~18°C) cinder slopes on the volcanoes. This contrast is best explained by differential heating from the morning sun. Figure 3 shows that where cinder fields and lava flows have similar topographic aspects, they also have similar radiant temperatures.

Only small temperature differences (<4°C) are evident between the low-albedo basalt flows near the valley floor and the high-albedo salt flats at the same elevation. The similarity is probably coincidental: The low-albedo basalt absorbs sunlight well, but because of its high thermal inertia (e.g., Gillespie and Kahle, 1977) most of the heat is conducted into the basalt, and its surface warms slowly. In contrast, the reflective salt flats absorb little energy, but because they have low thermal inertia, nearly all of it remains close to the surface, which warms rapidly. The similar surface temperatures of these different substances would probably not occur at most other times of day.

Streams, rivers and meadows appear dark in Figure 3. At ~1°C, the bodies of water are the coldest objects in this view of Owens Valley (snow in the mountains is at roughly −7°C). Their low temperatures result from evaporative cooling and also from the high heat capacity of water. Meadows are ~9°C, 19°C cooler than the adjacent scrublands. This great temperature contrast indicates the importance of phreatophytic vegetation in reducing air temperature in desert regions; the absence of similar large contrasts over scrublands shows the lesser influence of evapotranspiration there.

In general, the bajadas of northern Owens Valley are cooler than those at similar elevations to the south. This subtle southeastern temperature gradient occurs across the generalized boundary between the Great Basin and Mojave vegetation communities [Fig. 1b)]. However, the contrast is sufficiently small (<2°C) that it is difficult to detect in Figure 3.

There is also a T_s gradient across Owens Valley: the bajadas east of Owens River are cooler than those west of it. However, solar irradiation on the western, east-facing fans is greater at the midmorning time of TM image acquisition than on the eastern fans. This disparity ranges from ~10% for the gently sloping distal ends to 35% for the steeper fan heads. Additionally, the western bajada received sunlight earlier than the eastern fans, which were shadowed longer by the Inyo Mountains. Thus, the cross-valley gradient in T_s may not be apparent at other times of day, although the long-valley gradient should be.

Soils and Vegetation

Figures 4 and 5 show the endmember fractions for poorly developed soil and for vegetation, respectively, as calculated by the spectral mixture analysis of Part I. As calculated there, VF_s is a fraction related to the vegetation canopy projected onto the image plane according to the empirical equation

$$VF_s = -0.04 + 1.50 \text{ cover}, \qquad (1)$$

where "cover" is the fraction estimated in the field using line-intercept transects and where the scaling coefficient is particular to desert scrub on the bajada at the time and date of image acquisition (Part I, Table 4). The spatial patterns of the fractions of soil (Fig. 4) and vegetation (Fig. 5; cf. Part I, Fig. 6) on the bajadas are independent of one another and, as discussed in Part I, illustrate that edaphic variation is not the major factor controlling the distribution of vegetation there.

Soil variation on the bajada is controlled by rock type in the canyons associated with each alluvial fan, by age of the various depositional units of each fan, and by grain-size distributions that are increasingly dominated down-fan by fines. This variation can be seen in Figure 4, which shows that differences, represented by gray-level contrast in the young soil fraction image, are most prominent in a north–south direction, parallel to the axis of the valley. Secondary patterns in the soil fraction image radiate from canyons of the Sierra Nevada and White and Inyo Mountains. The distal ends of the fans are light and appear younger than the rest of the bajada, because of the accumulation of unweathered grus and sand downfan.

Soil variation on the valley floor is less organized than on the fans. In general, variability appears to be related to drainage patterns and ground-water distribution (Lee, 1912). Neverthe-

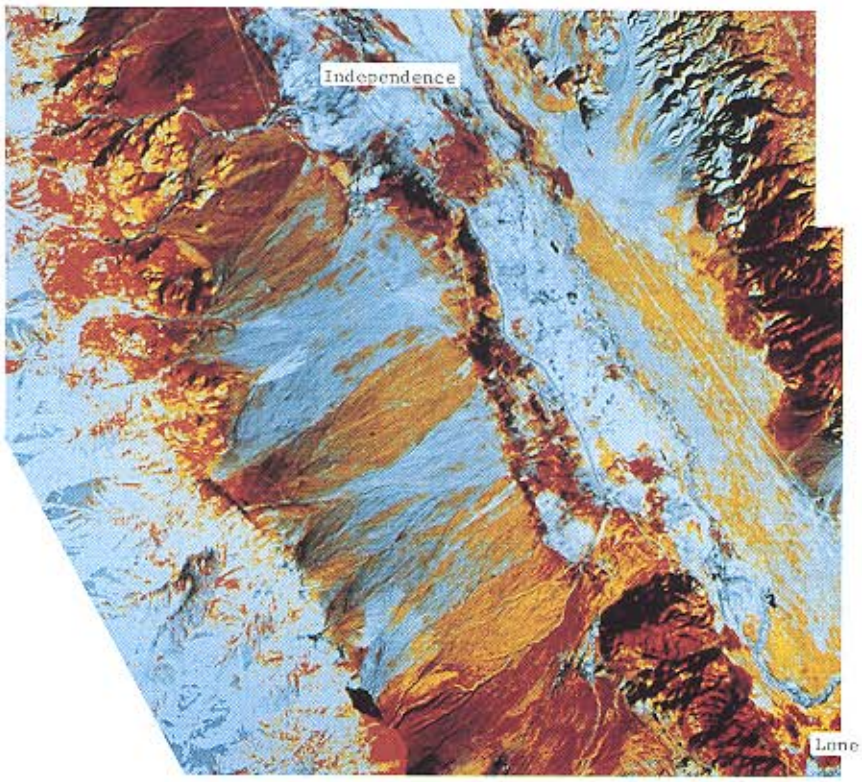

Figure 4. Color-contoured soil fraction image calculated from TM data and showing the proportion of each pixel, corrected for shading and shadow, which spectrally resembles the young soils on granitic sediments (Part I). Gray = <32%; yellow = 32–88%; red = >88%. The image is a subset of the southern part of the study area, enlarged to show detail. Lone Pine is at the bottom of the subset, and Independence is near the top. North is 11°ccw from "up"; image is ~50 km across.

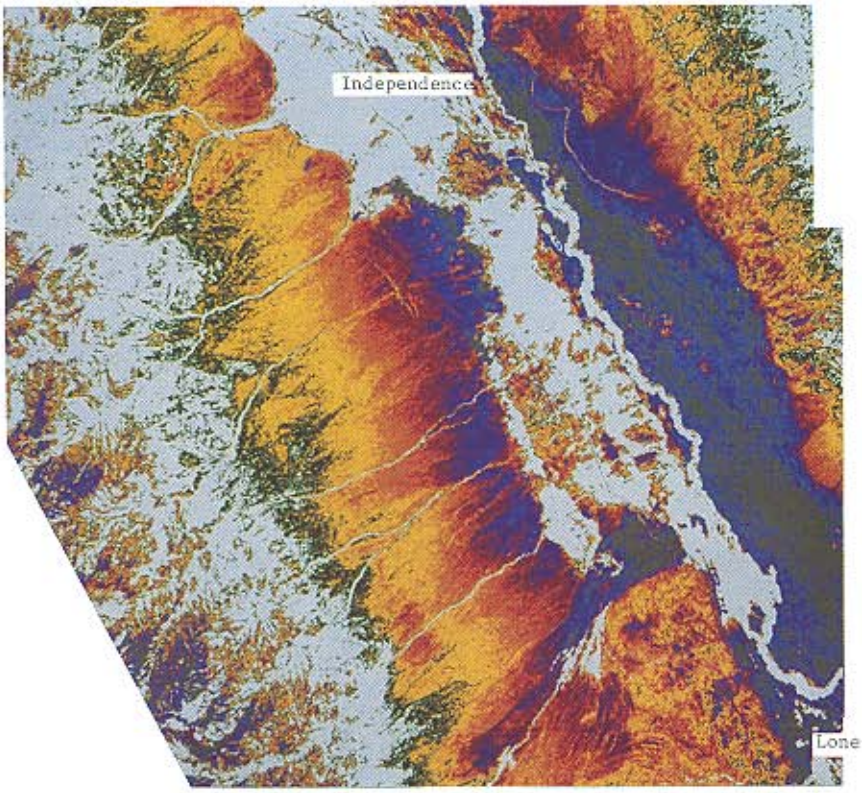

Figure 5. Color-contoured rescaled vegetation fraction (VF_s) image calculated from TM data and showing the proportion of each pixel, corrected for shading and shadow, covered by vegetation (Part I). VF_s is proportional to vegetation cover as measured in the field. Gray = 0–10%; blue = 10–20%; red = 20–30%; yellow = 30–40%; green = 40–50%; white = >50%. The image is the same subset shown in Figure 4.

less, regional patterns suggest an increase in the proportion of the poorly developed "young" soil from north to south, parallel to the axis of the valley.

Vegetation cover (VF_s) on the bajada (Fig. 5) is organized differently than the soils. The cover typically increases towards the Sierra Nevada range front, independent of the radial fan units but proportional to elevation. Regional gradients in vegetation cover are oriented east–west, perpendicular to the direction of maximum soil variation.

Exceptions to the east–west organization of the VF_s data are provided by unusual local edaphic conditions. For example, there are more grasses on the basalt flows of the Sierran bajada than on the granitic alluvium, resulting in high values of VF_s, at least in the spring. On the valley floor and at the base of a few alluvial fans, surface accumulations of evaporites support only sparse halophytic communities. In these nearly barren areas, VF_s is low. Also, near the fan heads old alluvial deposits are preserved that have dense impermeable soils which support only sparse desert scrub, and here VF_s is low also. A fourth example is the sparse community dominated by *Pinus longaeva* (Bristlecone Pine) on dolomite formations in the higher elevations of the White Mountains. In all these cases, edaphic conditions influence both vegetation cover and species composition, but these cases are exceptions to the typical pattern.

Figure 6. Image showing mean annual precipitation (MAP) isohyetal lines (Hollet et al., 1988) superposed on an "inverted" shade fraction image (Part 1). Numbers on isohyets are cm. MAP data were not available for the entire study area [Fig. 1a)]. The minimum MAP is displaced eastward from the center of Owens Valley, because of the rain shadow of the Sierra Nevada. Isohyetal lines are elevation-transgressive, with rainfall at constant elevation generally increasing northwards.

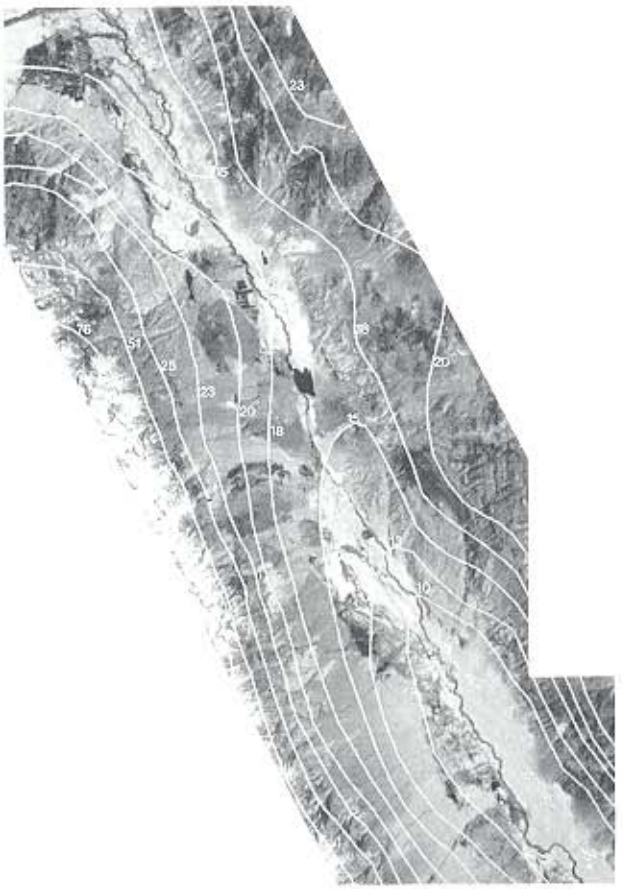

The densest vegetation on the fans of the Sierra Nevada occurs along streams. Here, willow, oak and cottonwood, together with a dense understory of rose, lupine, desert ceanothus, and gooseberry, replace the desert scrub. The riparian zone of phreatophytic vegetation is quite narrow: It is limited to roughly 10 m on either side of the streams. On the more arid fans of the east side of Owens Valley, the concentration of vegetation along streams is less noticeable. Here, in the rain shadow of the Sierra Nevada, the streams are generally ephemeral. Where permanent streams are found, the VF_s is higher, but the plants are typically sagebrush or other species of the Great Basin community that contrast with the surrounding scrub of the Mojave community.

Vegetation patterns on the valley floor are different than on the bajadas. Vegetation cover is densest in agricultural areas, and in the riparian areas near the Owens River and near springs and seeps. As for soils, the riparian areas reflect drainage patterns and ground-water distribution (Lee, 1912; Hollet et al., 1988).

MAP Data

Figure 6 shows the isohyetal map of Hollett et al. (1988) superposed on the complemented shade fraction image of the TM data [Part I, Fig. 4a)]. Although the isohyets were drawn from a sparse network of irregularly spaced measurement stations, the data in the vicinities of those stations are accurate and the major features of Figure 6 are considered reliable (W. R. Danskin, personal communication, 1989).

MAP ranges from ~100 cm at the Sierra crest down to ~10 cm on the floor of Owens Valley near Lone Pine. Upvalley, MAP increases to >15 cm near Bishop, although the increase in elevation from Lone Pine is only ~120 m. The isohyets are shifted eastward with respect to the valley floor, an expression of the rain shadow of the Sierra Nevada. At an elevation of 1500 m at the latitude of Red Mountain, the west side of Owens Valley receives 5 cm per year more precipitation than the east side, an increase of 50%.

The eastward "bulge" of isohyets near Crater Mountain occurs where foothills interrupt the Sierran bajada. This area is just across the crest of the Sierra from the canyon of the Middle Fork of the Kings River, one of the deepest canyons in North America. This major depression funnelled Pacific storms across the Sierra during the ice ages of the Pleistocene, resulting in a zone of lowered snow levels and enhanced glaciers (Burbank, 1990). Is the similar bulge in Figure 6 attributable to some effect such as the funnelling of modern storms, or is it merely a reflection of elevated terrain? Insight into these questions is one motivation for calculating the residual MAP image, which removes the strong first-order effects of elevation from the measured data.

Comparison of T_s, VF_s, and MAP

If a causal relationship exists between two among a number of covarying parameters, it may be possible to determine which pair is causally related by repeatedly regressing the variables pairwise over a large area. The causally related pair is likely to be the one with the least variability in the regression coefficients. It follows that the spatial patterns in images of causally related parameters will be more similar than if the parameters were only indirectly correlated. Figure 7 is one way of displaying the spatial consistency of patterns among vegetation, temperature, and mean annual precipitation. The black/white substrate of Figure 7 is the complemented shade fraction of the TM image, which basically contains topographic and location information. Superposed on the base are color-coded and contoured VF_s and T_s data [Fig. 7a)] and VF_s and MAP data [Fig. 7b)]. The brown and green zones in both Figures 7a) and 7b) are vegetation cover in the ranges of 12–20 and >20%, respectively. In Figure 7a), the light band cutting across the vegetation zones highlights T_s of 23–25°C. In Figure 7b), the light zone highlights MAP of 17–18 cm.

In Figure 7a), the green/brown contact in the vegetation data and the light band of the T_s data are concordant over most of the Sierran bajada from Bishop to Independence, but are discordant from Independence south to Lone Pine. On the bajada near Lone Pine, 12% vegetation cover is found immediately downslope from the highlighted isotherm, at temperatures near 25°C. Near Independence and north to Bishop, the 12% vegetation contour is far downslope from the highlighted isotherm, which has risen to the 20% isopleth near the fan heads. This discordant pattern is not observed on the eastern bajada. There, the

12% vegetation contour coincides with the 23–25°C isotherm nearly the entire distance from Lone Pine to Bishop. Thus the correlation between T_s and VF_s may be everywhere equally good, but the regression coefficients vary with latitude.

The 23–25°C isotherm is near the 1200-m elevation contour over most of the eastern bajada. On the western bajada the isotherm is at that same elevation near Lone Pine, but rises to the 1650-m contour north Independence. Because the western bajada receives more insolation than the eastern bajada at the hour of TM image acquisition, it is to be expected that the same isotherm occurs at a lower elevation on the west-facing fans. What is difficult to explain is the occurrence of the isotherm at the same elevation on both east-facing and west-facing slopes near Lone Pine.

In Figure 7b), the colored bands of VF_s data are concordant with the light band of the MAP data everywhere on the bajadas except near Big Pine, where the 17–18 cm isohyet is displaced to the east. The displacement is pronounced over the western bajada, where the 17–18 cm isohyet overlies the 12% vegetation isopleth. Elsewhere the same isohyet is near the 20% isopleth, on both sides of Owens Valley and regardless of latitude.

The 50% increase in MAP northward from Independence to Bishop is not reflected in the vegetation cover of the valley floor; instead, the

Figure 7. Color contour maps showing the discordance of vegetation cover and radiant temperature patterns, and the relative concordance of vegetation cover and mean annual precipitation patterns. The black/white image base is the complemented shade image (Part I). a) VF_s and T_s. The gray, brown and green zones correspond to <12%, 12–20%, and >20% vegetation cover, respectively; and the conspicuous light band corresponds to radiant temperatures of 23–25°C. The T_s image was smoothed using a low-pass 7×7 median filter. b) VF_s and MAP. The light band corresponds to MAP of 17–18 cm.

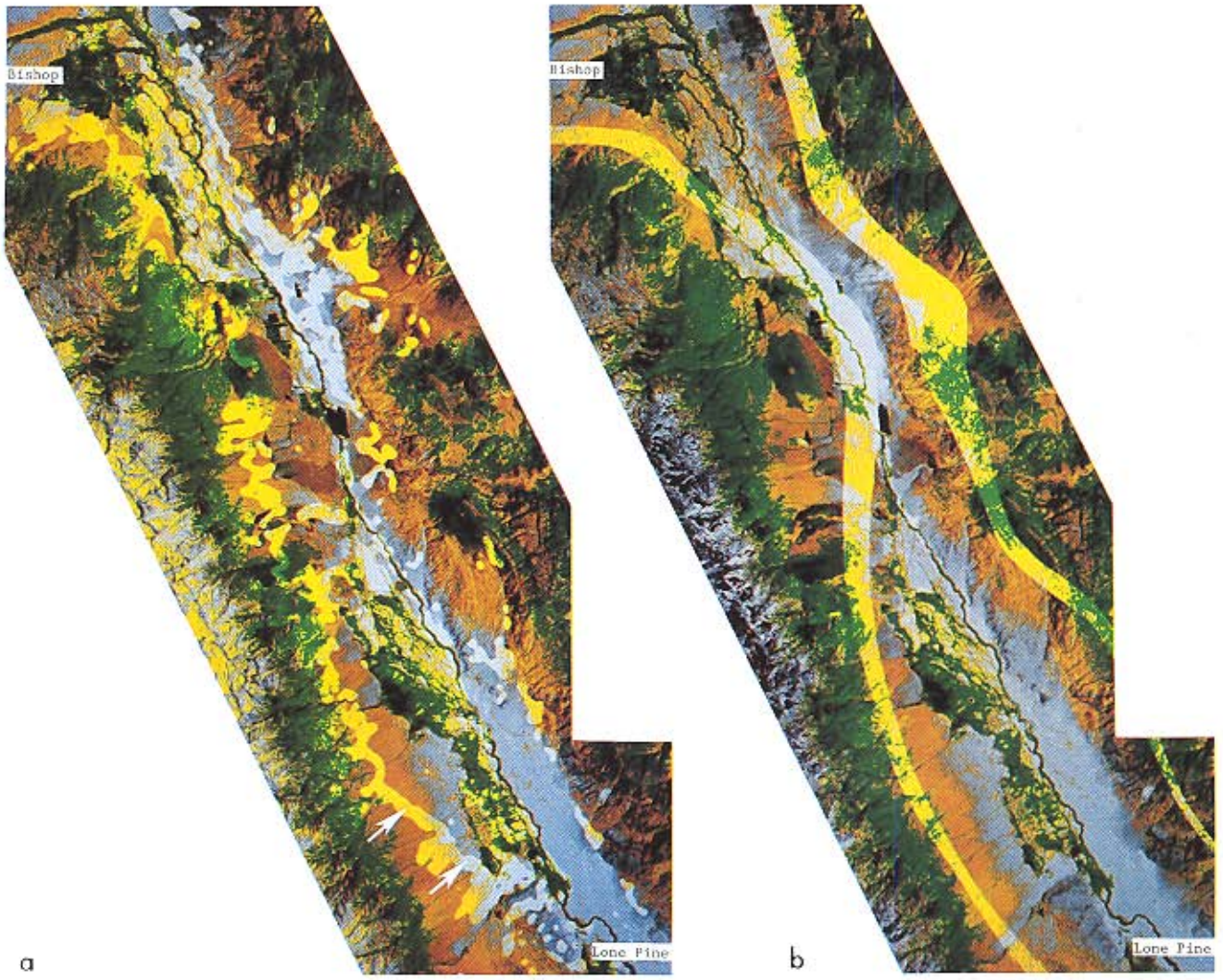

12% isopleth occurs everywhere near the base of the fans. In contrast, the 20% isopleth is elevation-transgressive, and is found at lower elevations at higher latitudes. Evidently at the base of the fans, vegetation cover is less well correlated with MAP than at higher elevations on the bajadas. The Mojave–Great Basin transition community gives way to Great Basin community [Fig. 1b)] roughly at the 15-cm isohyet (Fig. 6), at least on the bajadas. This transition also is discordant with the T_s contours [Fig. 7a)]. Significantly, the Mojave community is shifted eastward from the axis of Owens Valley, as is the MAP minimum locus but unlike the T_s data. The northern limit of creosote bush coincides closely with the 10-cm isohyet.

At every location, there is a general correlation between vegetation cover and T_s and between cover and MAP. As noted earlier, this correlated behavior is to be expected, because of the dominant influence of elevation on all three parameters. Furthermore, inspection of the T_s and VF_s data on fire scars showed that, at a local scale, T_s was controlled in part by vegetation. Figure 7 reveals the regional patterns of correlation between VF_s and T_s and between VF_s and MAP, but these patterns do not reveal a striking difference in the degree or consistency of correlation. Instead, cover on the upper fans appears to be consistently correlated with MAP, except on the western bajada near Big Pine; and cover appears to be consistently correlated with T_s, except on the western bajada near Lone Pine. Furthermore, the correlation between VF_s and MAP appears to break down on the lower bajada, and the correlation between VF_s and T_s is inconsistent across Owens Valley.

Clearly, comparison of the VF_s, MAP, and T_s data themselves is not sufficient to determine which relationships are causal. In order to investigate this question more fully, it is necessary to remove the strong influence of elevation from the data, so that areas of anomalous relationships may be better identified.

Temperature–Elevation Patterns

For the Sierran bajada from Big Pine to Lone Pine we observed high correlations among radiant temperature, elevation, and VF_s. Linear regression of temperature to elevation data was performed separately for each of 12 transects [Fig. 1a)], and variability among the coefficients was evaluated. The regression coefficients for the 12 transects are similar, and therefore the coefficients were recalculated for all the grouped 3329 measurements. Temperature can be estimated from elevation according to

$$\widehat{T}_s = 41 - 0.012\,E, \qquad (2)$$

where the regression coefficient $r = 0.87$. For the bajadas, the estimated temperatures range from ~20°C to ~26°C from head to toe. The transects are all on the Sierran bajada, with an eastern slope of ~2–4°. Therefore, the regression of Eq. (2) is strictly appropriate only for similar east-facing slopes under a similar cover of desert scrub.

T_s and elevation are linearly related only over a narrow range of elevations on the bajadas. If the transects of Figure 1a) are extended into the Sierra Nevada, the measured values of T_s are lower than predicted by Eq. (2), and higher-order terms are required to describe the convex pattern. In this, T_s differs from MAST and MSST, which are linear with elevation for all elevations in Nevada (Schimidlin et al., 1983).

Calculations of MSST for the bajada at 36.5° latitude, adjusted downwards 2°C, are ~27°C at 1200 m elevation to ~22°C at 1800 m elevation. At this location, MSST and T_s for the time and date of image acquisition are similar. However, the MSST gradient with elevation is -0.0077°C m^{-1}, significantly different from the gradient in Eq. (2), and T_s and MSST are not so close in the mountains above the bajadas. T_s and MSST agree best near the distal ends of the fans.

To determine the extent to which local temperature gradients on the bajada can be extrapolated to the geographic region, the variation in temperature associated with elevation (T_y) was removed from the temperature image. Figure 8 shows this residual temperature image. In Figure 8, dark areas are those cooler than predicted by elevation using Eq. (2). Lakes and reservoirs appear black. In neutral gray areas, observed values of T_s are in substantial agreement with predicted values. Much of Owens Valley is neutral gray; this is especially true on the bajadas. Light areas in Figure 8 are warmer than predicted from elevation; these areas are seen in the mountains as well as in Owens Valley. On the bajadas and valley floor, light areas generally are sparsely vegetated, whether because of range fires, unstable sandy substrate, or salt accumulation.

The overall low contrast and neutral gray tones in Figure 8 illustrate that the bajada temperature gradient of Eq. (2) is widely characteristic of Owens Valley, and that estimation of T_s using Eq. (2) is appropriate over the region. There is no appreciable asymmetry of gray tones about the axis of the valley (Owens River). Local departures from neutral gray in Owens Valley are caused by variations in surface orientation, surface albedo, soil moisture, and/or vegetation cover. West-facing or shadowed slopes, such as those of the Sierra canyons and of the west sides of the volcanoes, are darker than predicted, compared to sun-facing slopes at the same elevation. However, the west-sloping bajada east of Owens River is not appreciably darker than the Sierran bajada, despite the differential insolation noted above; thus, the sensitivity of the residual temperature image to small slope differences ($<10°$) is minor compared to the sensitivity to other effects.

The image patterns in Figure 8 enhance the topography of the Sierra Nevada, White, and Inyo ranges. The lower slopes of these mountains are lighter (Sierra Nevada) or darker (Whites, Inyos) than predicted from elevation, because of the effects of the sun-facing and shadowed slopes, respectively. At higher elevations, a sharp tonal boundary separates the lighter upper montane region from the darker lower slopes. In the Sierra Nevada but not in the ranges to the east, this

Figure 8. Residual temperature image, $T_s - \hat{T}_s$. $\hat{T}_s$ was calculated from TM and digital elevation data using regression coefficients defined for 12 transects on the Sierran bajada [Fig. 1a].

Figure 9. Residual vegetation cover image, $VF_s - \widehat{VF}_s$. $\widehat{VF}_s$ was calculated from TM and digital elevation data using regression coefficients defined for 12 transects on the Sierran bajada [Fig. 1a].

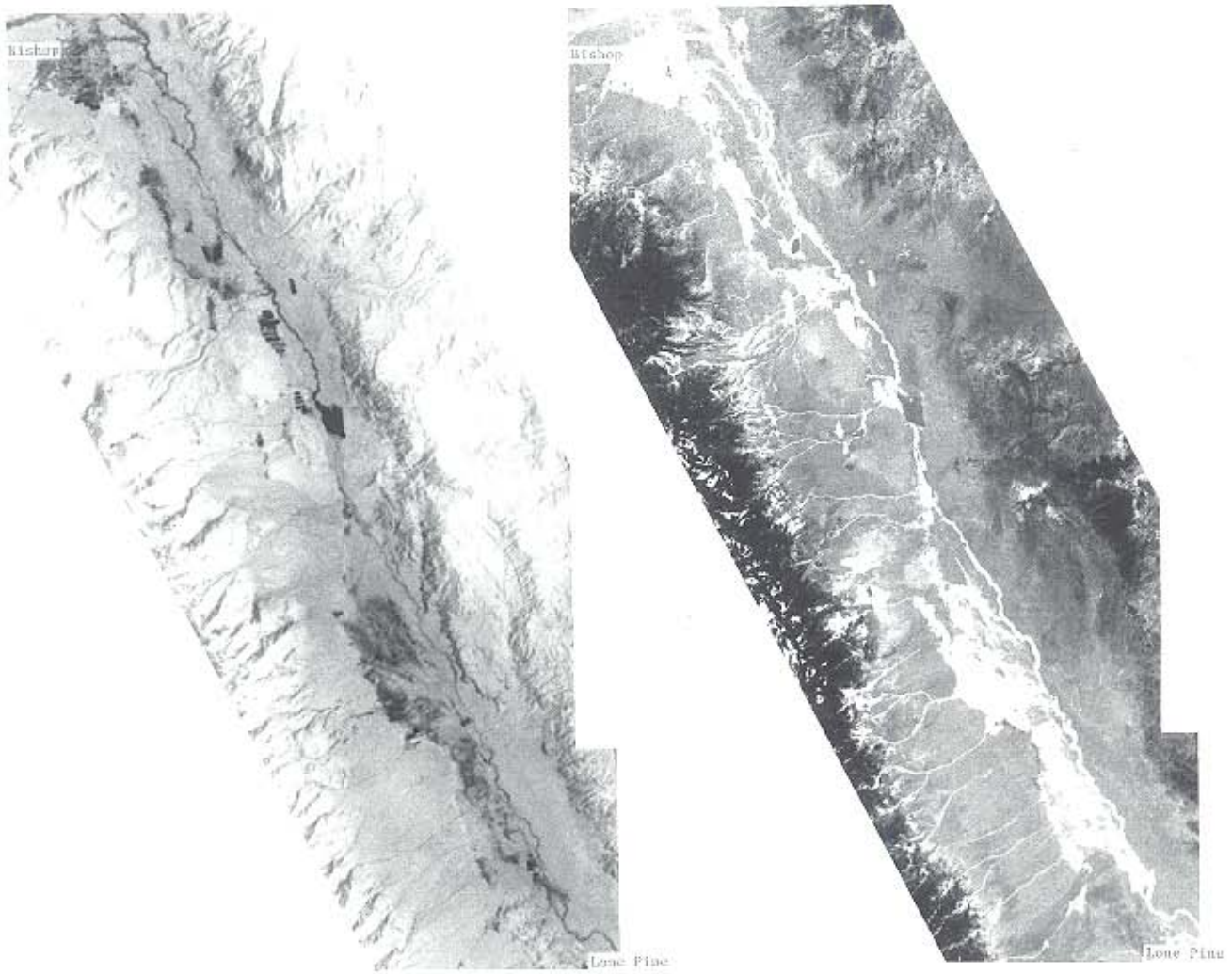

upper montane zone is truncated by cold snow fields.

Thus from Figure 8 we delineate three major temperature regimes in the Owens Valley area, corresponding to 1) the light zone within the montane regions of the Sierra, Inyo, and White ranges, 2) the foothills, alluvial fans, and parts of the valley floor, and 3) the riparian, irrigated, and high-groundwater environments within regimes 1 and 2.

The first regime is elevation-transgressive, and is discordant with the snowline which rises southward. Within this zone are significantly lower values of VF_s than on the upper bajadas. Vegetation is typically mixed conifers, with minimal understory. Inspection of aerial photographs and field observations suggests that the zone may be largely associated with the prevalence of sparsely vegetated talus slopes and bedrock cliffs.

The second temperature regime is on the foothills, the bajadas and the drier parts of the valley floor, where there is a strong correlation among elevation, VF_s, and temperature. This regime includes the Piñon–Juniper zone above the desert scrub, and extends into the mixed conifer forest in the mountains.

The third temperature regime corresponds to the phreatophytic environment. It has much lower temperatures than those predicted from the bajada transects, and thus appears dark in Figure 8.

There is a general correspondence between patterns in the VF_s image (Fig. 5) and in the residual temperature image, for the bajada and floor of Owens Valley. Areas of exceptionally dense vegetation, such as in the riparian zones, are associated with unusually low temperatures. In the residual temperature image (Fig. 8), the Bishop area, Owens River, and much of the valley floor west of the river are significantly darker than the bajadas (cooler than estimated). All of these dark areas in Figure 8 are wet or heavily vegetated (light in Fig. 5). Cultivated fields especially are darker than the surrounding surfaces in Figure 8. The agrarian areas are as much as 20°C cooler than nonvegetated areas on the valley floor.

Temperature differences on the bajadas (Fig. 3) correlate mainly with differences in elevation; variations associated with albedo (Fig. 2) are small. The thermal contrasts between the riparian and interfluvial slopes on the bajadas are less than those of the valley floor.

In contrast to the obvious general correspondence between patterns in the VF_s and $T_s - \widehat{T_s}$ images at lower elevations, in the mountains spatial correlations between patterns in Figures 5 and 8 are poorly developed, except for riparian areas in canyon floors.

The negative correspondence between VF_s and $T_s - \widehat{T_s}$ does not extend to the lava flows, which appear to be slightly more vegetated than the neighboring fans, but which are warmer than predicted from elevation alone. In Part I, we noted that the vegetation on the lava flows was dominated by annual grasses, which were still green by mid-May in 1985 (M. DeDecker, personal communication, 1986). Grasses on the valley floor produced a higher VF_s than equivalent cover of desert scrub (Part I, Table 4). The desert scrub cover on the lavas is ~40% less than the total cover indicated in Figures 5 and 7. Although grasses should have more evaporative cooling than desert scrub, evidently it is inadequate to overcome the heating due to the high R_n and the sparse cover.

Vegetation–Elevation Patterns

Regression of VF_s to elevation data for the same 3329 pixels on the 12 image transects showed that vegetation cover could be estimated from elevation according to

$$\widehat{VF_s} = -0.20 + 0.00027E, \qquad (3)$$

for which $r = 0.81$. Variability among the regression coefficients calculated separately was greater than for the regression of temperature against elevation, and the values in Eq. (3) were averaged from the separate analyses rather than from a single grouped analysis. The positive slope in Eq. (3) shows that vegetation becomes more abundant upslope on the fans, from $VF_s \approx 0.11$ at the toes to ~0.28 near the heads.

The residual image of $VF_s - \widehat{VF_s}$, which contrasts the observed vegetation cover and the cover estimated from elevation using Eq. (3), is shown in Figure 9. As with the residual temperature image, neutral low-contrast gray tones dominate much of Owens Valley in Figure 9, demonstrating that vegetation cover is well predicted from elevation there. In particular, the valley floor east of Owens River and much of the bajada have vegetation fractions close to those estimated from the se-

lected bajada transects. There is no obvious difference between the bajadas east and west of the Owens River.

The following areas have more vegetation than predicted by elevation, as indicated by light areas in the image: much of the west valley floor, the Owens River and other riparian areas, the city of Bishop, the basalt flows, and Crater and Red Mountains. The riparian environments on the bajadas are more distinct in the residual vegetation image than in the residual temperature image (Fig. 8). Cultivated areas are easily distinguished by their lightness and geometric borders. The lava flows and cinder cones were heavily vegetated at the time of TM data acquisition; however, they typically are covered with dry grasses by mid-May (Part I).

Recovering fire scars on the fans appear darker than unburned surrounding slopes, indicating less vegetation than predicted. Salt pans also have less vegetation than predicted, as does the valley floor east of Lone Pine.

Precipitation–Elevation Patterns

Regression of MAP to elevation data for the 12 image transects was performed, although the resolution of the interpolated MAP image was lower than that of the reduced TM data. The separately calculated regression coefficients were similar, and the data were grouped for a single analysis which related MAP to elevation according to:

$$\widehat{\mathrm{MAP}}\,(\mathrm{cm}) = -6.2 + 0.0147E, \qquad (4)$$

for which $r = 0.88$. The fit in Eq. (4) is improved somewhat with the addition of an E^2 term, but we use the linear regression for simplicity. The positive slope in Eq. (4) shows that precipitation increases upslope on the fans, from MAP $\approx$ 12 cm at the toes to ~22 cm at the heads.

A residual image of MAP $-\widehat{\mathrm{MAP}}$ was calculated by subtracting an image estimated from the digital elevation data and Eq. (4) from an image interpolated from the generalized contoured MAP data (Fig. 10). The most striking feature of the residual MAP image is the green zone of excess MAP over the Sierra Nevada. This zone would be reduced if a nonlinear regression had been used in Eq. (4). It is bordered on the east by a narrow deficient (gray) zone near the foothills and fan heads. The excess MAP of the Sierra Nevada is not seen over the Inyo range at comparable elevations; this is a consequence of the Sierra Nevada "rain shadow," in which there is reduced precipitation in the lee of the high mountains.

Most of Owens Valley north of Independence is in the yellow zone, indicating slightly enhanced MAP of 0–5 cm compared to the control transects. South of Independence, this yellow zone is restricted to the upper western bajada. This pattern shows that there is a general increase in "excess" MAP with latitude, which can be confirmed by inspection of Figure 6 for the valley floor, where there is little change in elevation. Finally, the prominent pink zone near Big Pine is a region of enhanced MAP (5–9 cm) that is imposed on the generalized latitude gradient. This zone is centered over the valley floor well away from the highlands of the Sierra foothills.

Thus actual values of MAP are well predicted from elevation for the Sierran bajada where the transects were taken, but they are underestimated to the north. This effect is maximum in the pink zone (Fig. 10) near Big Pine, where the isohyetal lines in Figure 6 bulge eastward. MAP data near this bulge are well constrained, because there are several measurement stations nearby (Hollett et al., 1988). Evidently, precipitation in the bulge is enhanced disproportionately to elevation, perhaps by storm funnelling, and the bulge is not simply a topographic effect. "Excess" MAP near the center of the bulge, ~15 km south of Big Pine, was ~5 cm.

MAP data are underestimated from elevation in the northern Owens Valley, compared to the southern valley. Excess MAP near Bishop was ~2.5 cm, less than near Big Pine but more than near Lone Pine (~ -1 cm). We attribute this regional pattern to a general increase of precipitation with latitude on the Pacific coast of North America. The altitude gradient in MAP for Owens Valley appears to ~4 cm/°.

MAP data are overestimated from elevation east of Owens River. MAP decreases from ~13 cm to ~9 cm from west to east over a distance of 16 km just south of Lone Pine. The gradient of 0.25 cm/km is greater than the latitude gradient by roughly a factor of four. This result is consistent with a deepening rain shadow east of the Sierra Nevada and is probably real, but the number of measurement stations is small (Hollett et al., 1988).

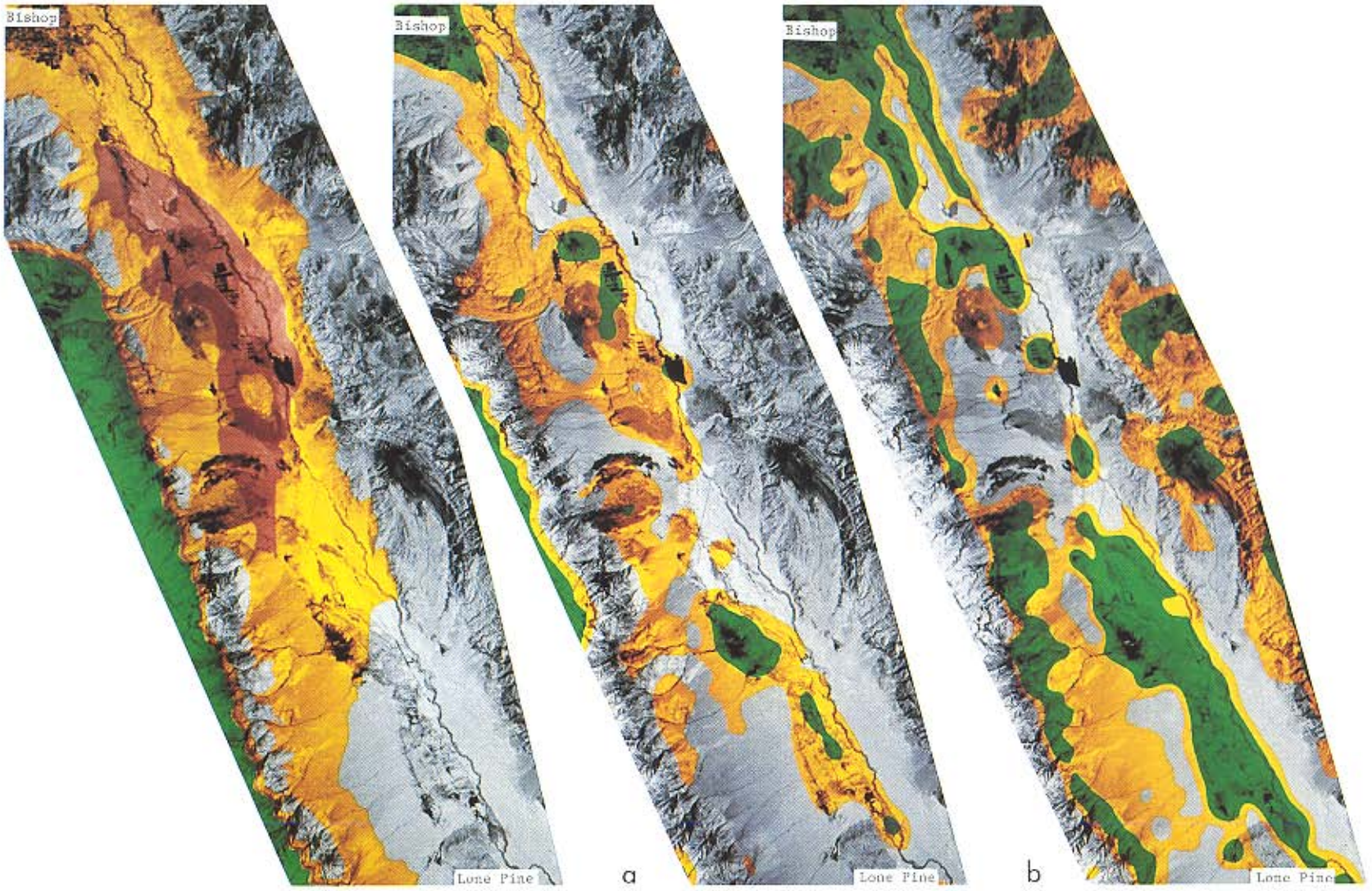

Figure 10. Contoured and color-coded image of residual mean annual precipitation, MAP − $\widehat{\text{MAP}}$. Data are draped over the complemented shade image. Gray areas have MAP anomalies of ≤0 cm; yellow areas are 0–5 cm; pink areas are 5–9 cm; and green areas are ≥9 cm. $\widehat{\text{MAP}}$ was calculated from generalized field measurements (Hollett et al., 1988) and digital elevation data using regression coefficients defined for 12 transects on the Sierran bajada [Fig. 1a)]. MAP data were not available for the entire study area [Fig. 1a)].

Figure 11. Color-coded, smoothed, and contoured images of residuals, for the part of the study area for which MAP data were available. Gray zones have "deficient" vegetation; yellow and green zones are areas of increasing "excess" vegetation, a) VF_s regressed to T_s, draped over the complemented shade image. Gray ≤0%; yellow = 0–12.5%; green > 12.5%. b) VF_s regressed to MAP, draped over the complemented shade image. Gray ≤ 0%; yellow = 0–17%; green > 17%.

If vegetation cover is proportional to precipitation, then the $VF_s - \widetilde{VF}_s$ image should show this same asymmetry, but if vegetation cover is controlled by temperature, then it should not. Likewise, the $VF_s - \widetilde{VF}_s$ image should reflect the precipitation excess near Big Pine if vegetation is proportional to MAP. Detailed comparison of the residual images is necessary to determine these relationships.

Comparison of the Residual Images

In general, the spatial patterns of the residual images of temperature, vegetation and precipitation (Fig. 8–10) are dissimilar. Large T_s residuals were associated with mountains, topographic shading, and riparian vegetation; VF_s anomalies were chiefly associated with ground-water and edaphic patterns on the valley floor; and MAP anomalies were associated with latitude, the Sierra rain shadow, and the "bulge" near Big Pine. If there exists a causal relationship between VF_s and MAP, or between VF_s and temperature, then these anomalies should coincide. Especially important are the anomalies associated with latitude, with the Sierra rain shadow, and with the excess precipitation near Big Pine. In order to investigate the hypothesized coincidences, we constructed color-coded, smoothed, and contoured residual images of VF_s regressed to T_s, and VF_s regressed to MAP [Figs. 11a) and b)]. The color-coded residual data were draped over the complemented shade image. Gray zones are areas where cover is well predicted from T_s or MAP, as measured in the transects of Figure 1a). Yellow and green zones are areas of "excess" vegetation.

Figure 11a) depicts the vegetation vs. temperature residual. The prominent features are moderate amounts of "excess" vegetation (yellow) over much of the western bajada, compared to the eastern bajada. Although this asymmetry across the valley may be attributed to rain-shadow effects (decreasing cover to the east), some or all of the effect may also be caused by low temperatures due to reduced insolation on west-facing fans in the morning.

The gray zone also encompasses the western bajada near Lone Pine; evidently T_s is reduced there, but cover is not. From Figure 7a) it appears that this effect is not related in a simple way to latitude, although there is an increase of yellow areas northward. The green zones concentrated on lava flows and on the valley floor are areas of much higher cover than predicted from T_s.

Figure 11b) is similar to Figure 11a), except that it depicts VF_s anomalies compared to MAP. The data are roughly organized in zones along the valley floor and the top of the western bajada. These zones, green in Figure 11b), are areas in which vegetation cover exceeds the amount predicted from MAP. Both zones are ones in which soil moisture is enhanced by proximity to ground water. In general, neither latitude nor rain-shadow effects are evident, and the excess precipitation in Big Pine "bulge" is matched by increased vegetation.

From the spatial covariance of vegetation cover and MAP over most of Owens Valley we infer that there is indeed a causal relationship between VF_s and MAP, and that vegetation abundance is controlled at least in part by precipitation and soil moisture. We have already established from inspection of local vegetation anomalies such as fire scars that a causal relationship appears to exist between T_s and VF_s, but we suspect that vegetation is influencing temperature, not the other way around. The discordance of temperature and vegetation isopleths near Lone Pine is evidence that VF_s is at most only secondarily influenced by T_s, because even the correlation there is poor. Finally, the discrepancy between vegetation cover and temperature in the rain shadow is difficult to evaluate with our data, because of differential insolation on the east-facing and west-facing bajadas.

Vegetation and Ground Measurements of Evapotranspiration

We compared remotely sensed vegetation cover data and ground measurements of ET in order to test the applicability of vegetation cover to estimating this important ecological parameter. Weather conditions during 16 May 1985 were stable with clear skies, and were similar to the preceding and following days. These conditions are favorable both for the determination of ET and for the remote estimation of vegetation cover. The ground determinations of ET for 16 May 1985 for the four Owens Valley stations ranged from <2 to >8 mm; annual ET ranged from 10 to 100 cm. The calculated daily ET values appear reasonable because maximum daily summer ET estimates for

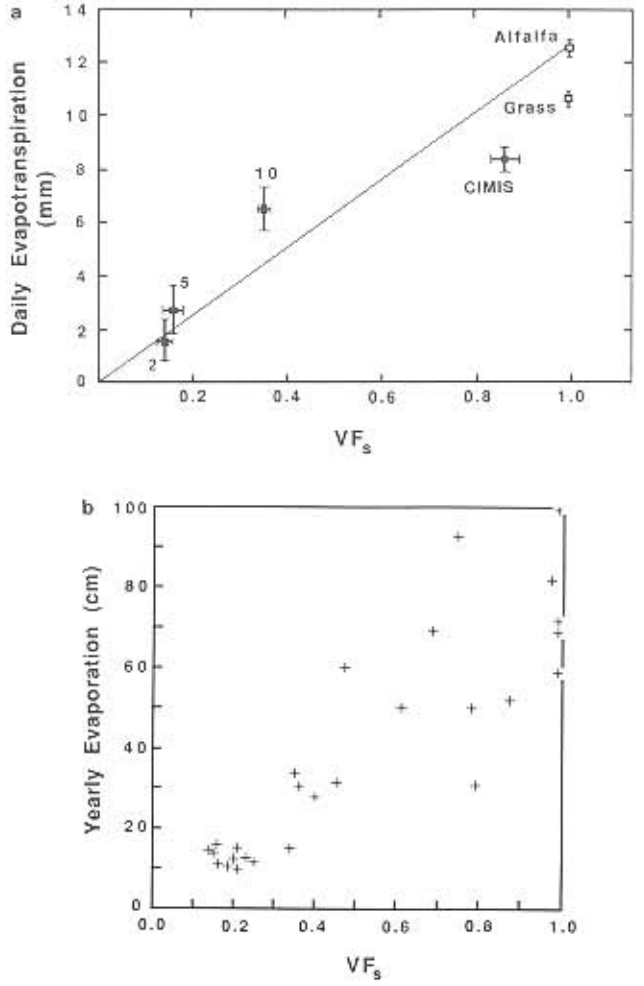

Figure 12. Variation diagrams relating VF_s estimates of ground cover and ET. The VF_s axis is calibrated in terms of ground estimates of vegetation cover. a) VF_s vs. ET on the date of image acquisition, based on hourly field measurements at four stations [Fig. 1a)]. For reference, maximum daily summer ET for fully irrigated standard tall grass and alfalfa are shown on the figure (100% cover). These estimates represent maximum ET rates found in southern California (Pruitt et al., 1987). The dotted line indicates the empirical limit of ET over the full range in cover. Error bars are ~±1 standard deviation; open boxes are reference data. b) VF_s vs. annual ET from coregistered sites on the valley floor (unpublished data from the Los Angeles Dept. of Water and Power, Rawson, personal communication, 1989). Vegetation canopy cover spans 0–100% for a range of community types, including Mojave-saltbush scrub, mixed-desert scrub and Great Basin sagebrush, and alkali meadow types. For reference, maximum annual ET for irrigated standard tall grass or alfalfa fields in southern California is 365 cm ± 10% (R. L. Snyder, personal communication, 1989). ET = 0.136 + 0.023 VF_s.

fully irrigated grass in southern California are 10–11 mm and for alfalfa are 12–13 mm (Pruitt et al., 1987).

In Figure 12a) we plot ground measurements of ET for 16 May against VF_s calculated from the TM data for the four corresponding areas on the valley floor. VF_s values range from ~0.1 to ~0.5. The calibrated cover estimates and daily ET data for the three sites covered by natural vegetation (#2, 5, and 10) appear to be linearly related, within the precision of the data. However, the data for the CIMIS station fall below a line drawn through the other data. Regression of a line to the data for all four stations shows that station #10 is the anomalous one, with the line passing within the error bars of the other data. Thus, in general, ET increases with VF_s, but there are too few data to establish if the relationship is linear.

Reference ET data for grass and alfalfa are also shown in Figure 12a). These are maximum values for fully irrigated grass and alfalfa, and they provide an empirical upper limit for possible ET rates. The data for site 10 lie above this limit; thus, it appears that site 10 has ET rates higher than expected for the calculated VF_s. Pixel-by-pixel examination of the VF_s values in the general vicinity of site 10 do not indicate significantly greater variance than for the 4×4 pixel neighborhood, and we therefore suspect that the ET value was overestimated.

The ET value for the CIMIS station is well below the empirical limit for alfalfa, as is the value for the standard irrigated grass plot. However, the CIMIS ET is within expected ranges if ET for the standard grass plot is accepted as the empirical maximum, rather than ET for the alfalfa. Unlike the other sites, the CIMIS station itself was unresolvable in the TM image, and its VF_s could not be measured directly. The CIMIS station was located within a larger irrigated pasture with $VF_s = 0.80$. VF_s for the carefully maintained station itself was probably greater than this value. Examination of irrigated pastures and alfalfa fields in the TM image indicate that 92% cover was the maximum in Owens Valley on the date of image acquisition, and this value must be an upper limit to cover for the CIMIS station too. Even using the lower limit of 0.80 for CIMIS cover in Figure 12a) does not alter the conclusions that CIMIS data fell under the empirical limit, and were similar to the data for the standard grass.

The vegetation at site 2, the CIMIS station, and the "control" grass and alfalfa are all single-layer canopies; sites 5 and 10 are single-layer canopy shrub communities. At this time we do not know what effect canopy architecture may have on the relationships of ET and VF_s. We expect that data from communities having complex multilayer

canopy structure may deviate from the linear relationships suggested in Figure 12a).

In Figure 12b) we plot area-averaged estimates of annual ET against VF_s. VF_s values range from ~0.1 to ~1.0. These data too are linearly related, with $r = 0.78$ [the regression equation is given in Figure 12b)]. Scatter about the regression line of Figure 12 may be due to misregistration of the image pixels with the field stations, errors in developing the ground ET model, inclusion in ground ET calculations of annuals not present at the time of the satellite overpass, and to errors in the calculation of VF_s. Given the range of vegetation types in the 32 land units represented in Figure 12b), it is also possible that different ET–cover relationships are appropriate for the various communities.

DISCUSSION

Instantaneous Measures and Virtual Parameters

We have compared data of several different kinds in an effort to understand the environmental influences on vegetation in Owens Valley. R_n and T_s both were calculated from TM images; thus, they are instantaneous looks at net radiation and radiant temperature, respectively. Soil fraction and VF_s images were derived from the TM images using spectral mixture analysis. Elevation and MAP images both were created by interpolating contour maps. The elevation image represents instantaneous measurements of topography, but the MAP data are averages of measurements made over several years.

The above images differ fundamentally in the temporal stability of the measured parameters. At one end of the stability spectrum, T_s represents a parameter that varies hourly, daily, and seasonally. T_s is not an intrinsic property of the scene, although it depends in part upon such intrinsic properties as albedo and thermal inertia. R_n is likewise variable, although it too is dependent upon albedo. VF_s is an instantaneous measure of vegetation cover, which is a relatively stable intrinsic component of the scene. We found that vegetation endmembers were the same for the May and December TM images; however, the VF_s estimates for desert scrub cover decreased by 11% from Spring to Winter (Part I). Even for deciduous perennials and ephemerals, VF_s estimates change little from week to week. This stability is due in part to the normalization by the shade fraction, which removes the first-order dependency of the radiance data upon lighting geometry. The R_n image, comparably normalized for shade (and corrected for topographic shading) might be converted into a stable image of albedo.

At the other end of the spectrum, the MAP data are inherently stable because they are a statistical summary of years of measurements. MAP will change only on a time scale longer than the period of measurement. The elevation image is the least changeable of all, because topography changes little even on the time scale of centuries.

We regard the TM-derived images, at a basic level, as instantaneous measures of rapidly and slowly varying phenomena expressed directly by the interaction of electromagnetic radiation and the earth's surface. This may not be a useful viewpoint for the field geologist or ecologist, but many of the parameters of concern to them are only indirectly expressed in radiance images and may be difficult to measure directly. If remotely sensed data of some kind covary with the parameter of interest, then they have been regarded as proxy data. Measuring one allows the other to be inferred.

In special instances, the instantaneous measurements may serve not only as proxy data, but also as estimates of "virtual" parameters. We define virtual data as having a spatial distribution similar to the parameter of interest at the moment of interest, even though the moment of interest and data acquisition are different. A virtual measure is an instantaneous measurement that if repeated sufficiently would at some time be a proxy for the desired measurement. The concept of the virtual measure is important to the discussion below.

The T_s Image

Radiant temperature is an estimate of the kinetic temperature only of the immediate surfaces of the elements that comprise a scene. Thus it is only an effective or model temperature if there is a strong temperature gradient at the surface, or if the scene is not homogeneous at the pixel scale. Most scenes at the midmorning time of TM overflight are warming rapidly, and have strong temperature gradients. Furthermore, most scenes are heterogeneous at the pixel scale. This is especially true of

Owens Valley (Part I, Fig. 2). The radiant temperature measured by TM is mixed from the temperatures of sunlit and shadowed soil, rock, and litter, from the trunks and branches of standing vegetation, and from the green leaves. Thus, T_s cannot be regarded exactly as a kinetic temperature.

The surface temperature of each element of the scene is dependent on the surface albedo and incident solar radiation. Surface temperature is strongly affected by the transport of heat by the wind and the evaporation of moisture from soils and vegetation. Thus, we might expect T_s to be approximated by the ground radiance, mixed with the radiance from cooled leaves. However, field studies have shown that the temperature of desert scrub is the same (± 1°C) as the air temperature (Kahle et al., 1984). Even if the sparse desert scrub vegetation is actively transpiring, the effect on air temperature is minor: The volume of cooled air is small and soon mixed by the wind with the larger volume of uncooled air. Thus, T_s over the Owens Valley bajada is a composite measurement of instantaneous surface and air temperatures.

Figures 2 and 3 show that R_n, which is proportional to albedo and which therefore should covary with the substrate temperature component of T_s, is considerably more variable over the bajadas than is T_s. R_n is responsive to mapped lithological units having different albedos, but T_s is not. Strictly, T_s is proportional to the logarithm of R_n, but even an image of R_n stretched logarithmically has more variance than the image of T_s. Thus, it appears that T_s must be controlled by the vegetation temperature disproportionately, or that T_s is a proxy for air temperature, at least over the bajadas. This could occur if the air temperatures on the morning of acquisition rose more rapidly and were higher than the ground temperatures.

Even if T_s were a proxy for instantaneous air temperature, how can it be related to the temperature controls on vegetation envisioned by the ecologist? Vegetation is generally taken to be sensitive to maximum or minimum temperatures. These values are not directly related to the instantaneous T_s, and can only be established by repeated measurement over a long period of time.

We propose that even if T_s is only an instantaneous measurement, its spatial distribution in Owens Valley is nevertheless of ecological interest, and furthermore that T_s is a virtual measure of the annual maximum temperatures that interest the ecologist. Not all images of T_s would satisfy these requirements. The TM image used in this study was acquired at 9:50 a.m. Images taken at other times of day or at different seasons would have different patterns of shading and shadow, which would change the local values of T_s. For example, T_s for the December TM image discussed in Part I showed very little variation over the entire Owens Valley. Patterns in this image bear little resemblance to patterns in the May T_s image; thus, the significance of the two images must be different.

Vegetation and Edaphic Factors

The VF_s measurement is well suited to show the relationship between vegetation cover and soil type, as it is relatively insensitive to species composition. At regional scales in the Owens Valley the cover of vegetation as measured by VF_s is largely independent of soil composition, except on the valley floor, where high ground water and evaporites both exert strong local controls on community and total cover. On a regional scale, cover on the valley floor is different from cover on the bajadas, which can be seen from the coincidence of the 12%-cover isopleth and the valley floor–bajada contact over much of the eastern side of Owens Valley. Unlike isopleths farther up the fans, which parallel MAP isohyets, the 12% isopleth is discordant with MAP data. Thus it appears that at the regional scale, the cover at the distal ends of the fans (and on the valley floor) is not controlled by precipitation, but by stronger edaphic and groundwater influences.

At local scales there are other exceptions to the above generalization where species or communities have adapted to specific edaphic niches. Even in these edaphic niches, the vegetation cover remains close to that of the regional surroundings. These results suggest that the overall vegetation cover on the bajadas is limited mainly by environmental factors that operate on a regional scale. Of the regional factors implicated in controlling vegetation, the most important in Owens Valley appear to be soil moisture and temperature.

Vegetation, Soil Moisture, and Temperature

At the regional scale the Sierra Nevada rain shadow limits the amount of direct precipitation in most parts of Owens Valley to <20 cm per year (Fig. 6). Soil water comes from a combination of precip-

itation and groundwater runoff from the mountains (Hollett et al., 1988), but only close to streams and on the valley floor is runoff the dominant component. There, the abundance of soil moisture is reflected in the dense communities of phreatophytic species. Elsewhere the cover of desert scrub decreases down-fan, parallel to the Sierra Nevada range front. This pattern does not reflect the radial organization of substrate and soil units of the alluvial fans, but is similar to the distributions of the three interrelated parameters: elevation, precipitation, and temperature. Another pertinent observation is that the vegetation cover on the distal ends of the fans is much more variable than elsewhere on the bajada, ranging from ~5% to 15%. This variability cannot be attributed to regional patterns of temperature or precipitation distribution; it must be due to differences in soil permeability and soil moisture.

We separated the intertwined variables of vegetation cover, temperature, soil type, and precipitation by comparing the coarse spatial distributions of each parameter, assuming that direct causal relationships would be revealed by close correspondences of these patterns, and that indirect relationships would be revealed by discordant patterns or trends. This information would not be evident from regressions of the variables measured at single sites or transects, because of the high degree of correlation of all the variables. Comparison of the spatial distributions of the variables is a more sensitive measure because it is responsive to variability in the degree of correlation, or in the regression coefficients. Using this approach, it was immediately apparent that vegetation cover on the bajadas is largely independent of edaphic control, for example.

Three lines of evidence indicate that temperature does not control the amount of vegetation on the bajadas: 1) the bases of the fans are nearly uniform in temperature, whereas the vegetation cover is highly variable in these areas; 2) in the north end of Owens Valley on the east side there are steep alluvial fans and valleys where there is little increase in vegetation with altitude, although temperatures decrease over these same areas; and 3) on the Sierran bajada from Lone Pine to Independence, T_s contours are discordant with VF_s contours, whereas contours of VF_s and mean annual precipitation are more concordant. This concordance appears to be true, regardless of the coarse nature of the MAP data grid.

On balance, we found that MAP, not T_s, appeared to be consistently correlated with vegetation cover on the bajadas. Thus, our analysis supports the findings of Shimeda (1985) and Beatley (1984) that precipitation controls vegetation cover. However, our findings do not rule out temperature as an important factor, especially since the actual midmorning temperatures represented in the T_s image are not representative of the seasonal extremes (although we suspect that the T_s patterns are representative of the spatial distribution of temperature maxima). The general correspondence of vegetation and temperature anomalies is not sufficient to establish firmly that vegetation and temperature are causally related in the bajada and nonphreatic communities on the valley floor; nevertheless, it appears that precipitation, and hence soil moisture, is the most important influence limiting vegetation abundance on the bajadas. On the valley floor, soil type and proximity to ground water exert the strongest influence on vegetation type and cover.

Beatley (1984) has suggested that annual extremes of air temperatures limit the northward spread of species of the Mojave community [Fig. 1b)], and, in particular, that minimum temperatures are the limiting factor for creosote bush. We find that the Mojave community is shifted eastward from the axis of Owens River, similar to the eastward shift of the precipitation minimum due to the Sierra rainshadow, but unlike the more symmetric patterns of T_s. The northern limit of creosote bush is near Independence [Fig. 1a)] and corresponds roughly to the northern extent of the 10-cm isohyet of MAP. The December T_s image shows little variability over the valley floor and bajadas, unlike the May T_s image. If the December T_s image is representative of the spatial distribution of minimum temperatures, it is clear that there is little correlation between the distribution of minimum temperatures and the Mojave community. The above observations are evidence that the main factor limiting the Mojave community may be precipitation instead of temperature, although our findings are not conclusive.

Vegetation, Temperature, and Evapotranspiration

In the absence of satellite images taken at multiple times of day we have assumed that the spatial

pattern of T_s in our TM image represent the relative spatial distribution of temperatures throughout the day, except for regions of high relief subject to shadowing. There is precedent for the assumption that single instantaneous thermal measurements can be used to estimate diurnal temperature curves. Instantaneous temperatures have been used to estimate daily-to-monthly total ET for irrigated agriculture, based on the difference between radiant surface temperatures and air temperature (Hatfield et al., 1983; Jackson et al., 1983; Klaassen and Van den Berg, 1985; Seguin and Itier, 1983; Soer, 1980; Choudhury et al., 1986; Taconet et al., 1986). Such methods could not be applied in our study because of the significant terrain relief, because of the low vegetation cover with underlying soils of varying albedos and because of the difficulty of measuring air temperature remotely.

The strong positive correlation between VF_s and ET (Fig. 12) indicates to us that VF_s, a measure of vegetation cover that changes little over the year, can be used as a proxy for estimates of daily and annual ET. Evapotranspiration in desert scrub communities is a variable phenomenon, peaking daily in the early morning and seasonally when there is the most moisture available (Caldwell and Ehleringer, 1985; Ehleringer, 1985). If VF_s is to be used as a proxy for ET, then it is necessary to note that the ET referred to is not an instantaneous value, but rather an estimate of the long-term or integrated amount of evapotranspiration. We call VF_s a measure of *virtual* ET, to keep this distinction in mind. A more detailed treatment of the relationship between VF_s and ET is the subject of a forthcoming article (Ustin et al., in preparation).

SUMMARY AND CONCLUSIONS

We have evaluated five environmental factors in Owens Valley as they affect the abundance and distribution of vegetation: net radiation, temperature, elevation, precipitation, and soil type. We conclude that, on the regional scale of a 150-km-long segment of the valley, the vegetation cover is controlled primarily by the mean annual precipitation. Generalized differences in soil type and proximity to ground water on the valley floor cause a regional difference in vegetation cover between the bajadas and valley floor. At local scales, ground water and edaphic factors exert significant influence on vegetation cover. Temperature does not appear to be the major influence on vegetation at either regional or local scales within the valley, although this generalization probably does not hold throughout the montane areas. There is, however, clear evidence that vegetation influences the temperature in a major way in riparian areas, and to a minor extent on the bajadas, through evapotranspiration.

The boundary between Mojave and Great Basin vegetation communities is roughly concordant with the precipitation isohyets in both the southern and the northern parts of Owens Valley, and it does not correspond to isotherms or to isopleths of the other environmental variables that we considered. Perhaps the Mojave–Great Basin ecological transition is governed by the mean annual precipitation rather than by direct or indirect effects of temperature.

Our results highlight the importance of spatial scale in studying the distribution of vegetation. Vegetation abundance and mean annual precipitation are seen to be generally coincident only on the regional scale. At local scales the amount of vegetation may be highly variable, depending on local availability of surface water and soil type. Viewing the vegetation abundance from one or a few local areas can lead to erroneous conclusions as to the overall causative environmental factors. In Owens Valley it is not appropriate to assume that point measurements or observations can be extrapolated to regional scales. Instead the local conditions commonly are the exceptions that demonstrate the regional "rule."

We suggest that in Owens Valley the regional distribution of vegetation as measured by VF_s with suitable calibrations, can be viewed as a map of mean annual precipitation and as a map of "virtual" evapotranspiration. Thus, the regional VF_s pattern appears to be a good indicator of the present-day climate. Local departures from the overall distribution of VF_s are apparent, and do not obscure the broader pattern. It may be possible to use VF_s to measure climatic patterns in other arid and semiarid areas.

The results presented in this paper depend on an accurate measurement of sparse vegetation cover under conditions of variable soil backgrounds. In Part I we gave a detailed account of a

new method for assessing sparse vegetation using a spectral mixing model. In this paper we have shown that the TM thermal band, used in conjunction with VF_s derived from the visible and near-infrared bands, provides critical data for evaluating the environmental influences on vegetation abundance. The Landsat TM system is unique in that the six visible and near-infrared bands are generally adequate for measuring VF_s and the thermal band is coregistered and acquired at the same time. Our results suggest that TM data are especially useful for investigating vegetation in arid lands in terms of the spectral, spatial coverage, and that the approach used in Owens Valley may be broadly applicable to other desert areas.

We appreciate the assistance of the staff and the use of facilities at the University of California White Mountain Research Station. We thank P. Novak an the Los Angeles Department of Water and Power for providing us with a vegetation map of the Independence Quadrangle. We thank M. DeDecker for her assistance in plant identification and help in understanding the ecology of the region. We thank the U.S. Geological Survey for precipitation and micrometeorological measurements, and L. Duell, the U.S. Geological Survey and the California Irrigation Management Information System, for daily ET estimates. We thank D. Groeneveld and R. Rawson for annual ET estimates from their studies of the valley floor vegetation, and R. Snyder for reference ET data. We thank S. Willis for support with image analysis, K. T. Paw U for critical reviews of an early manuscript, and P. Shippert and D. Nitsch for assistance with graphics. Thanks to G. Vogler for layout and final presentation of graphics and images. This research was partially supported by NASA Grant NAS7-918 and Jet Propulsion Laboratory Subcontract 956899, and NASA Grants NASW 4016 and NASW85 to the University of Washington. We gratefully acknowledge the W. M. Keck Foundation for computer equipment and support.

REFERENCES

Beatley, J. C. (1974), Effects of rainfall and temperature on the distribution and behavior of *Larrea tridentata* (Creosote-Bush) in the Mojave desert of Nevada, *Ecology* 55:245–261.

Beatley, J. C. (1975), Climate and vegetation patterns across the Mojave/Great Basin transition of southern Nevada, *Am. Midl. Nat.* 93:53–70.

Billings, W. D. (1949), The shadscale vegetation zone of Nevada and Eastern California in relation to climate and soils, *Am. Midl. Nat.* 42:87–109.

Burbank, D. W. (1990), Late Quaternary snowline reconstructions for the southern and central Sierra Nevada, California: re-assessment of the Recess Peak Glaciation, *Quat. Res.*, forthcoming.

Caldwell, M., and Ehleringer, J. (1985), Cold deserts, in *Physiological Ecology of North American Plant Communities* (B. F. Chabot and H. A. Mooney, Eds.), Chapman Hall, New York, pp. 198–212.

Choudhury, T. N., Idso, S. B., and Reginato, R. J. (1986), Analysis of a resistance-energy balance method for estimating daily evaporation from wheat plots using one-time-of-day infrared temperature observations, *Remote Sens. Environ.* 19:253–268.

Ehleringer, J. (1985), Annuals and perennials of warm deserts, in *Physiological Ecology of North American Plant Communities* (B. F. Chabot and H. A. Mooney, Eds.), Chapman Hall, New York, pp. 162–180.

George, W., Pruitt, W. O., and Dong, A. (1985), Evapotranspiration modeling, in *CIMIS Final Report 10013-A* (R. L. Snyder, W. O. Pruitt, E. W. Henderson, and A. Dong, Eds.), U.C. Land, Air, and Water Research Paper Series B53812, pp. 3.36–3.61.

Gillespie, A. R., and Kahle, A. B. (1977), The construction and interpretation of a digital thermal inertia image, *Photogramm. Eng. Remote Sens.* 43:983–1000.

Goldberg, D. E., and Turner, R. M. (1986), Vegetation change and plant demography in permanent plots in the Sonoran desert, *Ecology* 67:695–712.

Groeneveld, D. P., Warren, D. C., Hubbard, P. J., and Yamashita, I. S. (1986), Transpiration processes of shallow groundwater shrubs and grasses in the Owens Valley, CA, Phase #1: Steady state conditions, Inyo County, Bishop, CA, 130 pp.

Hastings, J. R., and Turner, R. M. (1965), The changing mile; an ecological study of vegetation change with time in the lower mile of an arid and semiarid region, Univ. of Arizona Press, Tucson, AZ, 317 pp.

Hatfield, J. L., Perrier, A., and Jackson, R. D. (1983), Estimation of evapotranspiration at one time-of-day using remotely sensed surface temperatures, *Agric. Water Manage.* 7:341–350.

Hollett, K. J., Danskin, W. R., McCaffrey, W. F., and Walti, C. L. (1988), Hydrogeology and water resources of Owens Valley, California, U.S.G.S. Water-Supply Paper 2370-B, 118 pp.

Jackson, R. D. (1984), Total reflected solar radiation calculated from multi-band sensor data, *Agric. For. Meteorol.* 33:163–175.

Jackson, R. D., Hatfield, J. L., Reginato, R. J., Idso, S. B., and Pinter, P. J. (1983), Estimation of daily evapotranspiration from one time-of-day measurements, *Agric. Water Manage.* 7:351–362.

Jackson, R. D., Pinter, P. J., and Reginato, R. J. (1985), Net radiation calculated from remote multispectral and ground station meterological data, *Agric. For. Meteorol.* 35:153–164.

Jarvis, P. G., and McNaughton, K. G. (1986), Stomatal control of transpiration: Scaling up from leaf to region, *Adv. Ecol. Res.* 15:1–49.

Kahle, A. B., Shields, J. P., and Alley, R. E., (1984), Sensitivity of thermal inertia calculations to variations in environmental factors, *Remote Sens. Environ.* 16:211–232.

Klaassen, W., and Van den Berg, W. (1985), Evapotranspiration derived from satellite observed temperatures, *J. Clim. Appl. Meteorol.* 24:412–424.

Lee, C. H. (1912), An intensive study of the water resources of a part of Owens Valley, California, U.S.G.S. Water-Supply Paper 294, 135 pp.

MacMahon, J. A., and Wagner, F. H. (1985), The Mojave, Sonoran, and Chihuahuan deserts of North America, in *Hot Deserts and Arid Shrublands, Ecosystems of the World* (M. Evenari and I. Noy-Meir, Eds.), Elsevier, Amsterdam, vol. 12, pp. 105–202.

MacMahon, J. A., and Wiebolt, T. F. (1978), Applying biogeographic principles to resource management: A case study evaluating Holdridges Life Zone Model, in *Intermontane Biogeography: A Symposium* (K. Harper, Ed.), Great Basin Natl. Mem., vol. 12, pp. 245–257.

Merriam, C. H. (1898), Life zones and crop zones of the United States, *U.S.D.A. Div. Biol. Surv. Bull.* 10:9–79.

Price, J. C. (1981) The contribution of thermal data in Landsat multispectral classification, *Photogramm. Eng. Remote Sens.* 47:119–236.

Pruitt, W. O., Fereres, E., Kaita, K., and Snyder, R. L. (1987) Reference ET (ET_0) for California, University of California Bull. 1922, Div. Agricultural and Natural Resources, 13 pp.

Schmidlin, T. W., Peterson, F. F., and Gifford, R. O. (1983), Soil temperature regimes in Nevada, *Soil Sci. Am. J.* 47:977–982.

Schreve, F. (1912), Cold air drainage, *Plant World* 15: 110–115.

Schreve, F. (1934), Vegetation distribution related to runoff, rainfall, and soil moisture, *Assoc. Am. Geogr. Anal.* 24:131–156.

Seguin, B., and Itier, B. (1983), Using midday surface temperature to estimate daily evaporation from satellite thermal IR data, *Int. J. Remote Sens.* 4:371–383.

Sellers, W. D., (1965), *Physical Climatology*, Univ. of Chicago Press, Chicago.

Shelford, V. E. (1963), *The Ecology of North America*, Univ. of Illinois Press, Urbana, IL, 610 pp.

Shimeda, A. (1985), Biogeography of the desert flora, in *Hot Deserts and Arid Shrublands, Ecosystems of the World* (M. Evenari and I. Noy-Meir, Eds.), Elsevier, Amsterdam, vol. 12, pp. 23–77.

Smith, P. D. (1987), Use of evaporation pan (Epan) data to estimate evapotranspiration (ET): i.e., Crop water use, U.C. Agricultural Extension, Bishop, CA (unpublished open file report), 2 pp.

Smith, M. O., Ustin, S. L., Adams, J. B., and Gillespie, A. R. (1990), Vegetation in deserts: I. A regional measure of abundance from multispectral images, *Remote Sens. Environ.* 31:1–26.

Snyder, R. L., and Pruitt, W. O. (1985), Estimating reference evapotranspiration with hourly data, in *CIMIS Final Report 10013-A* (R. L. Snyder, W. O. Pruitt, E. W. Henderson, and A. Dong, Eds.), U.C. Land, Air, and Water Research Paper Series B53812, pp. 7.1–7.3.

Soer, G. J. R. (1980), Estimation of regional evapotranspiration and soil moisture conditions using remotely sensed crop surface temperatures, *Remote Sens. Environ.* 9:27–45.

Taconet, O., Carlson, T., Bernard, R., and Vidal-Madjar, D. (1986), Evaluation of a surface/vegetation parameterization using satellite measurements of surface temperatures, *J. Clim. Appl. Meteorol.* 25:1753–1767.

Waring, R. H., Aber, J. D., Melillo, J. M., and Moore, B. III (1986), Precursors of change in terrestrial ecosystems, *Bio. Science* 36:433–438.

West, N. E. (1983a), Overview of North American temperate deserts and semi-deserts, in *Temperate Deserts and Semi-Deserts* (N. E. West, Ed.), Elsevier, Amsterdam, pp. 321–330.

West, N. E. (1983b), Great Basin-Colorado Plateau Sagebrush semi-desert, in *Temperate Deserts and Semi-Deserts* (N. E. West, Ed.), Elsevier, Amsterdam, pp. 331–350.

West, N. E. (1983c), Colorado Plateau-Mojavian Blackbrush semi-desert, in *Temperate Deserts and Semi-Deserts* (N. E. West, Ed.), Elsevier, Amsterdam, pp. 399–411.

Wilson, D. H., Reginato, R. J., and Hollett, K. J. (Eds.) (1989), Evapotranspiration measurements of native vegetation, Owens Valley, CA June, 1986, USDI Geological Survey Water Resources Div. Proj. 42618, Open File Report.